9-26-2023

FUNDAMENTAL STUDY OF IONIC LIQUID PHYSICOCHEMICAL EFFECTS ON THERMAL STABILITY OF MODEL BIOLOGICAL MACROMOLECULES

Austin Keith Clark
Rowan University

FUNDAMENTAL STUDY OF IONIC LIQUID PHYSICOCHEMICAL EFFECTS ON THERMAL STABILITY OF MODEL BIOLOGICAL MACROMOLECULES

by

Austin Keith Clark

A Thesis

Submitted to the
Department of Chemistry and Biochemistry
College of Science and Mathematics
In partial fulfillment of the requirement
For the degree of
Master of Science in Pharmaceutical Sciences
at
Rowan University
September 8, 2023

Thesis Chair: Timothy D. Vaden, Ph.D., Professor, Department of Chemistry and Biochemistry

Committee Members:
Gregory A. Caputo, Ph.D., Professor, Department of Chemistry and Biochemistry
Chun Wu, Ph.D., Associate Professor, Department of Chemistry and Biochemistry

Dedications

To my mother, father, and brother for always supporting me on this path and your unconditional love, thank you.

Acknowledgments

To reach this precipice of learning, a task such as this one is never completed alone. I would first like to begin by acknowledging everyone who has helped me achieve the completion of this degree. Starting with my mentor and guide Dr. Timothy D. Vaden, whom, without his help, I would not have had the necessary tools, knowledge, and passion to reach for this degree. Thank you for your guidance, dedication, and patience in leading me down this path which I had only dreamed of achieving, you mean a great deal to my life and future, and for that I cannot thank you enough. Secondly, I would like to thank all the educators I had the pleasure of meeting and learning from across the 18 years of schooling it took to achieve this goal. Every educator played a role in shaping me into who I am today, and I cannot thank you all enough for your kindness and dedication to your students, of which I was lucky to be one. I would like to especially thank all the Rowan Department of Chemistry and Biochemistry faculty and staff for their support.

I would also like to acknowledge the people who helped me complete this research, directly or indirectly. Those include but are not limited to Vaden Research Group students, both graduate and undergraduate 2019-2023, and those students outside of Vaden Research Group that provided support and someone to relate to while navigating this program. I would like to thank all the technical staff of Rowan University Department of Chemistry and Biochemistry, for all their research knowledge and assistance with instruments and resources. I would also like to acknowledge my friends, old and new, who have helped me to learn and grow and become the person I am today.

Abstract

Austin Keith Clark
FUNDAMENTAL STUDY OF IONIC LIQUID PHYSICOCHEMICAL EFFECTS ON THERMAL STABILITY OF MODEL BIOLOGICAL MACROMOLECULES
2021-2023
Timothy D. Vaden, Ph.D.
Master of Science in Pharmaceutical Sciences

Ionic Liquids (ILs) are substances with a unique physical attribute compared to that of solid ionic salts. At room temperature, ILs are molten salts that have a variety of physical effects that can play a role in their impact on other molecules, as solvents or solutes. They can play the role of the solvent in a variety of applications, from biofuels to organic catalysis or as excipients in pharmaceutical formulations. These ILs have a desirable use as solvents due to their ability to be tunable substances. Changing the cation or anion of the IL causes a change in its physical effects on other molecules that interact with it. The understanding that intermolecular forces play a large role in the IL's physical properties is well understood. But there are a plethora of cation and anion combinations to form molten ILs and these interactions are rarely one size fits all regarding their impact on biological substances. The focus of this thesis is on the physicochemical effect of biologically compatible, or environmentally friendly, ILs' impact on a set of model biological macromolecules. The understandings gleamed from the results lead to a subset of ILs and their impact on a subset of model biological structures to be applied to future study and therapeutic applications.

Table of Contents

Table of Contents (Continued)

List of Figures

List of Figures (continued)

Figure Page

List of Figures (continued)

Figure Page

List of Tables

Chapter 1

Introduction

Section 1 Introduction and Literature Review

Section 1.1 Proteins

Proteins are specific macromolecules with highly evolved structures and functions; they cannot easily be mimicked by small-molecule drugs or other chemicals. Proteins require a large amount of energy to be synthesized by the cell from the DNA that encodes them. Based on the Human Proteome project, there are more than 20,000 different genes that code for proteins in human cells.[1] Consequently, there are 20,000 different protein structures in human cells, for example, those involving structural cell support and signaling for cell functionality. Further protein structures arise from post translational modification, folding or cleavage errors, or amino acid mutations improperly coded in the DNA. With so many different steps for error in the protein synthesis pathways, there are possibilities for too much, too little, or misshapen proteins that lead to disease. For example, the CFTR protein misfolding leads to cystic fibrosis, as well as some cancers which some therapeutics have involved protein therapeutic intervention. For the reason of protein specific disease, there are many different types of protein therapeutics,[2 3], biomarkers,[4] and interventions.[5 6 7]

According to Leader et. al, proteins are naturally synthesized in the body and will have a low possibility of eliciting an immune response and causing stress or harm to the recipient because of their specificity.[2] This makes proteins perfect therapeutic targets. While successful protein therapies do not typically elicit an immune response, it is still

possible that some proteins may be seen as foreign substances and elicit an immune response from studied proteins that fail as therapies. Also, some proteins, due to their hydrophilic or hydrophobic residues can lead to an issue entering the cell or through therapeutic delivery. This knowledge leads to the understanding that solvents and excipients play a large role in protein therapeutic delivery and utilizing other substances to aid in delivery would be useful research.

Use of protein therapeutics is necessary for disease intervention and research has been done on protein therapeutics for decades.[2] For example, insulin was discovered to be the protein that is necessary for signaling to the body that it needs to start sugar metabolism processes. For many people with diabetes, insulin is a necessary therapeutic because their body is missing this protein.[2] With the large increase in protein technologies and therapies, it is more important now than ever to understand the fundamental interactions of excipient, solvent, or delivery molecules that could interact with these proteins to keep them in a stable state for study, increase shelf life, or improve therapeutic delivery. One option to lead to an improved impact of these technologies would be the use of ionic liquids (ILs) for their tunable physicochemical effects. [8 9 10]

This thesis focuses on understanding how ILs affect model proteins. There are various choices of model proteins available. Protein structure, ease of availability/purification, or cost can affect these choices. A good model protein is one that has a structure that might be shared by many proteins to apply the learned knowledge fundamentally for better understanding. The model proteins of choice for these studies were azurin and mCherry. Azurin is a good model protein as it has a mixed structure and is easily available. Another good option for study is mCherry, as it has a large β-barrel

structure which is a great model for understanding interactions with strong tertiary structures. Methods for synthesis and purification are well known.[11]

Azurin and mCherry are also easy to study and understand from a spectroscopic standpoint. Azurin is a copper redox protein involved in the denitrification process of *P. aeruginosa* and has a mixed structure, containing both β-sheets and α-helices.[12] This structure can be seen in Figure 1.1, from the protein database (pdb), showing the β-sheets and α-helices, with the oxidized Cu^{2+} as a blue ball in the core of the protein.[13] The single tryptophan residue is present in the structure and represented by the red ball. Trp is a naturally occurring amino acid with an environmentally sensitive fluorescence. When excited at 285 nm, the Trp in azurin gives rise to fluorescence emission at 308 nm, indicative of a properly folded structure. Alternatively, if the protein is denatured, the Trp is exposed to the solution and the solvation effects of water red shifts the emission to 355 nm. Example of these folded (308 nm) and unfolded (355 nm) spectra can be seen in Figure 1.2.[13]

The protein mCherry was also chosen as a model protein for studying IL effects because it has a different tertiary structure than azurin. The mCherry protein has a large β-barrel structure which is structurally stable. The mCherry protein also has a chromophore which can be seen in the center of the mCherry structure in Figure 1.3 and has an absorbance at 579 nm. The protein structure is easily identified with its CD spectrum, seen in Figure 1.4. The identifiable characteristics of the mCherry CD spectrum are the two positive peaks at 265 nm and 345 nm. These wavelengths are a result of the secondary structure of the mCherry, so when these peaks go to zero, it can be thought of as unfolded mCherry protein. There is also a negative peak at 579 nm on the

CD spectrum and this is a result of the chromophore absorbing light. Using the technique of CD spectroscopy, which is outlined in section 3, to identify the mCherry protein is useful as it can help us identify if the chromophore is being affected by IL independently from the rest of the secondary structure.

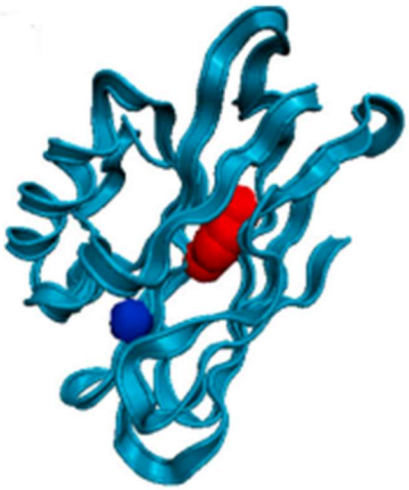

Figure 1.1. Azurin protein structure from the protein database (pdb) showing both α-helices and β-sheets. The Cu^{2+} ligand is a blue ball, and the red ball is the single tryptophan residue in the protein.

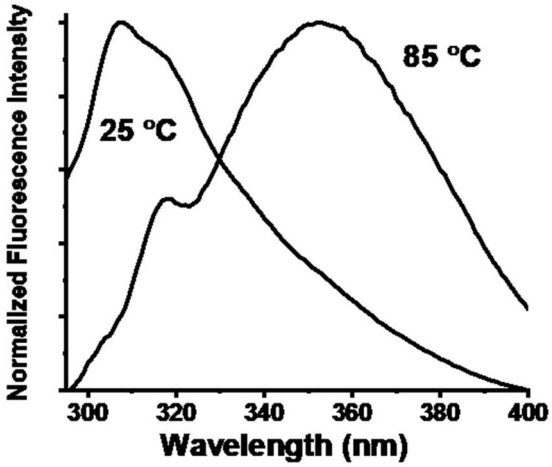

Figure 1.2. The fluorescence spectra of both folded and unfolded azurin after excitation at 285 nm; folded protein is indicated by the peak at 308 nm and 25 °C while unfolded protein is indicated when the fluorescence red shifts to 355 nm at higher temperatures.

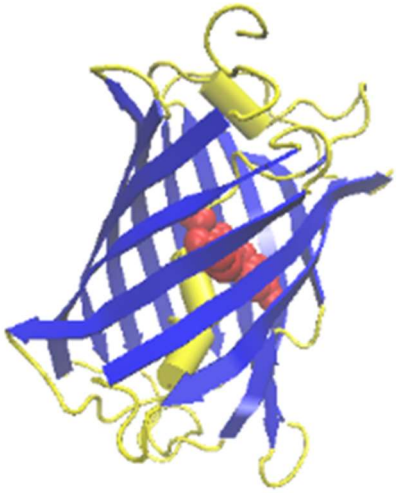

Figure 1.3. The VMD structure of the mCherry protein being studied, the chromophore can be seen in the center of the structure (red) as well as the β-barrel structure (blue).

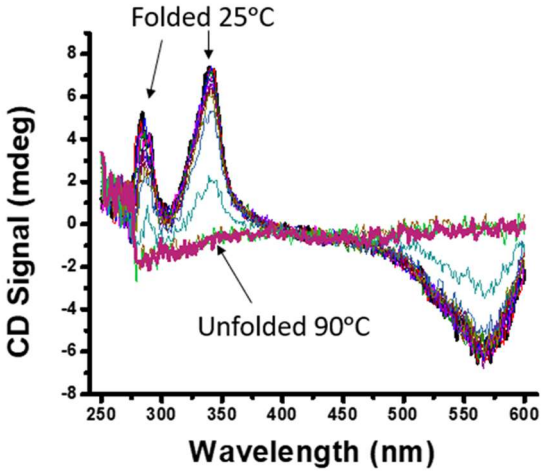

Figure 1.4. CD spectra of mCherry in the presence of 0.5 M ChPhe and 1 mg/mL mCherry in PBS pH 7; the peak at 579 nm comes from the chromophore of mCherry, the positive and negative peaks being present indicate folded protein, and flat CD signal indicate unfolded protein.

Section 1.2 Ionic Liquids (ILs)

ILs are molten salts at room temperature that are known to have various physicochemical effects in a variety of applications.[9 14 15 16 17 18 19] One such application is their usefulness as an excipient, solvent or delivery material for protein or DNA therapeutics.[9 18 19] Before they are used with therapeutics, the IL physicochemical effects should be further understood.

ILs were reported as far back as 1912, and knowledge on their interactions and usage has been growing since.[20] As stated before, ILs are ionic substances that are liquid at room temperature and typically have a viscous consistency. This arises from the fact that the ionic interactions between the cation and anion are not strong enough to form a solid crystal lattice at room temperature so instead they remain and exist together in liquid form.[21 22 23] Ionic interactions prevent them from being a liquid that flows very easily, which gives rise to the increased viscosity. This has allowed ILs to be substances coined as "designer solvents" because the cation and anion can be changed to tune the desired properties.[10] The applications that arise from ILs depend on the ions used for cation and anion. Aprotic ionic liquids (AILs) are ILs that have low solubility in water and range from pyridinium to imidazolium cations and typically are paired with a halide group, like tetrafluoroborate or chloride for example. [10] Protic ionic liquids (PILs) are ILs that consist of Brønsted acids or bases and typically have a proton transfer occur to form the strong ionic interaction.[10] PILs have seen application in the field of fuel cell technologies as solvents and proton transfer interactions.[10]

There are various subcategories of ILs in these previously mentioned categories (PILs, AILs, etc.) ILs have many different physicochemical interactions with a broad distribution of molecules, polymers, or other substances, the focus in this thesis will be more biologically centered.

1.3 G-Quadruplex DNA and RNA

It is known that DNA/RNA structures are comprised of the building blocks of five polar nucleic bases. The bases consist of pyrimidines: cytosine, thymine, and uracil; as well as purines: guanine and adenine. These nucleobases are bound to a deoxyribose/ribose sugar which is connected to a phosphate group. These nucleotides are connected via negatively charged phosphodiester backbone to form the DNA/RNA strand. It is well known that these DNA/RNA sequences commonly form a helical secondary structure (known as a topology). While this is the most common form of DNA/RNA, the knowledge of other secondary structures that DNA/RNA can take has been understood for over 50 years.[24] [25] One such structure is the G-quadruplex (G4) formation of DNA/RNA. A G4 tetrad is comprised of 4 guanine base pairs from the same DNA/RNA strand on the same tetrahedral plane. These base pairs can form 2 Hoogsteen hydrogen bonds with another guanine nucleotide as well as form π-π stacking interactions to help stabilize the tetrad. Each guanine can be both an acceptor and donator for a Hoogsteen hydrogen bond with an adjacent guanine nucleotide.[25] [26] [27] The 6^{th} oxygen atom in the guanine base pairs is responsible for coordinating with the metal cation (K^+, Na^+, or Li^+) present in the core of the G4 DNA, allowing further stabilization of the molecule. The metal coordinating cation pulls these oxygens away from the base pairs allowing for stabilization of the Hoogsteen H-bonds. The conformation of the G4 tetrad

can vary based on 5' and 3' directionality upon folding. This is what leads to parallel, antiparallel, or hybrid structures.[28] [29]

There are various biological roles that G4 DNA/RNA take on, dependent on their location in the sequence.[30] [31] G-quadruplex DNA typically occurs at the telomeres of chromosomes and in some cancer cell lines.[32] [33] Without these structures, it is possible for the DNA to unravel or even express at a time when it is not necessary for expression to occur. These structures are typically stable on their own and can be denatured by enzymes such as telomerases.[24] [26] [34] When cells are healthy and maintain these telomerases at a normal level for replication, there are typically no problems, and the telomeres are released to allow normal gene expression.[24] [26] When cells are unhealthy and over express these telomerases, it is possible for them to destabilize the G-quadruplex structures leading to cancerous cell lines.

For these reasons, stabilizing the G-quadruplex structure is a useful technique for containing and preventing cancerous cell lines from forming. There are many kinds of drugs used to stabilize the G-quadruplex structures to reduce the formation of different cancers. One of the most relevant and recent drugs that have been found to easily bind to and stabilize the G-quadruplex structures are porphyrin-based drugs.[35] These porphyrin rings are cationic and have a high affinity for the guanine tetrads. They can bind at the top, bottom, or sides of the G-quadruplex.[35] One such porphyrin drug was TMPyP4 or α,β,γ,δ-Tetrakis(1-methylpyridinium-4-yl)porphyrin p-toluenesulfonate. This drug is well known to bind to G-quadruplex structures and stabilize it to reduce the possibility of cancerous cells forming. Previous work has shown that imidazolium chloride ILs can reduce the binding of TMPyP4 to G-quadruplex DNA.[35]

The amount of cancerous cell lines is wide and growing. Some examples include the c-MYC, $B16_m$ and others which form different types of cancers.[26] The c-MYC cell line is a popular target for G4 study as the G-quadruplex structures are commonly found in these cell lines. In the c-MYC oncogene, there is a section of the strand upstream of the c-MYC promoter region known as the nuclease-hypersensitive element III_1 (NHE) that is known to account for 75-85% of the total transcripted c-MYC oncogene.[36] Regulating and preventing the expression of this MYC transcription factor is useful for reducing cancer formation. This can be done with the use of small molecule drugs like the porphyrin drug, TMPyP4, to stabilize the G-quadruplex structure found in the telomeres of MYC cell lines.[35] There are many studies to support the study for this topic.[32 34 35]

The structure of G-quadruplex DNA can be seen in Figure 1.5A where the guanine base pairs are labeled with a "G", the tetrads are represented in purple, and the direction of the DNA strand is signified by the arrows. Another VMD representation of the G-quadruplex DNA structure can be seen with K^+ represented by the yellow balls (Figure 1.5B) and without K^+ (Figure 1.5C). The selected G-quadruplex DNA strand for this thesis was the c-MYC oncogene Pu22, which was commercially purchased from GenScript and can be seen in Figure 1.6. This DNA sequence is what forms the structure in Figure 1.5A. The different topologies that are possible with G-quadruplex DNA can be seen in Figure 1.7 where the parallel, anti-parallel, and hybrid topologies are shown respectively at the bottom of Figure 1.7.[28] The sequence from the Pu22 oncogene utilized was found to form the parallel topology based on the CD spectrum related to other sources.[37 38] There would be value to have knowledge of the physicochemical effects of

various ILs interacting with the G-quadruplex DNA. The ILs used in this DNA study can be seen in Figure 1.8 below.

G-quadruplex RNA is a very similar structure to G-quadruplex DNA. The few differences are that RNA contains an extra oxygen atom on the 2' carbon on the ribose backbone of the nucleotide, as well as the replacement of thymine to uracil in RNA sequences. G-Quadruplex RNA structures are another useful model molecule for testing ILs. This is because of the wide array of applications ranging from genetic regulation to RNA vaccine technologies.[39] [40] There has been some study of ILs with RNA structures and there is promise in the use of ILs to stabilize RNA in forms that are less stable.[41] [42] It is known that RNAses cause an increase in destabilization of RNA structures, but not DNA structures.[43] This is an important understanding for handling of RNA during research as well as storage and delivery issues. Use of G-quadruplex RNA is another model molecule like G-quadruplex DNA useful for gaining further understanding how ILs interact with the structure.

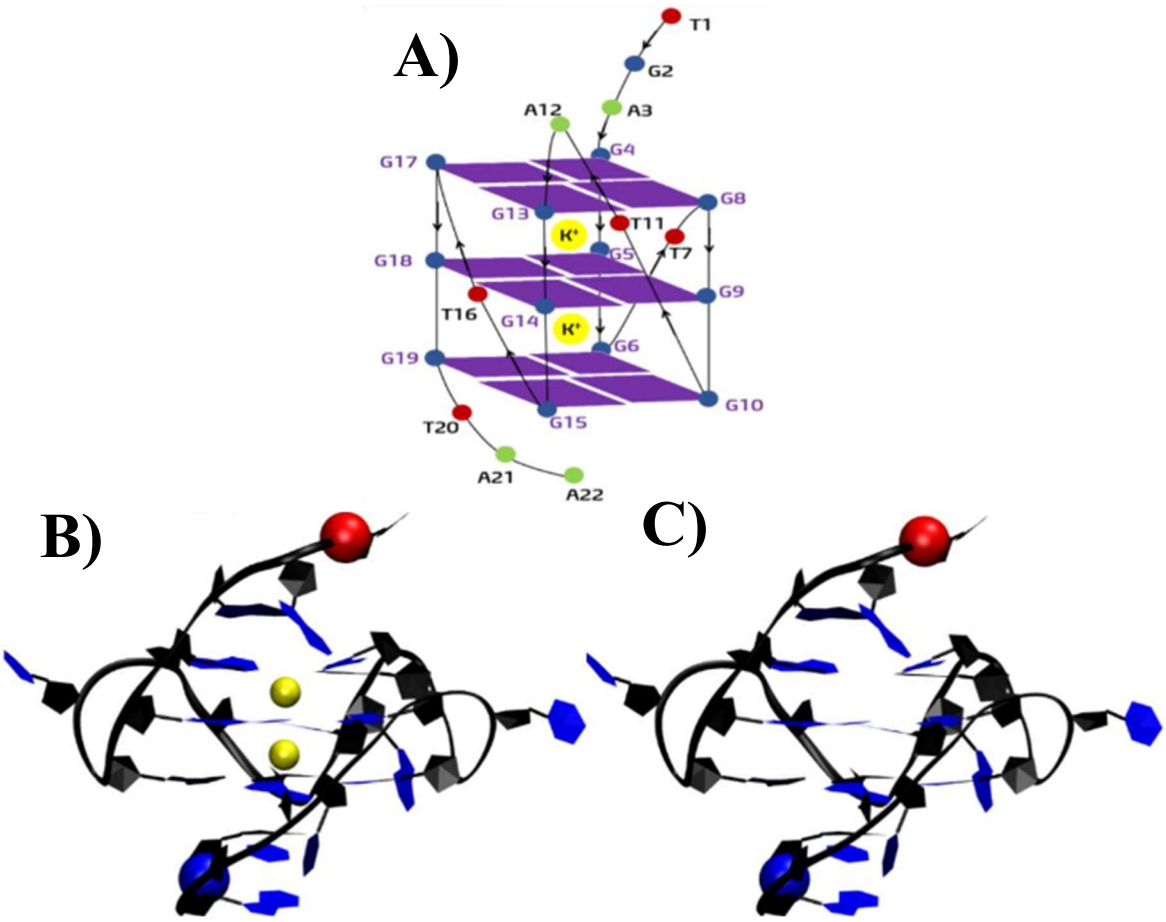

Figure 1.5. This figure shows a (A) cartoon representation of the Pu22 DNA folded into the G-quadruplex form and a (B) simulated VMD G-quadruplex DNA with K^+ and C) without K^+.

5′-TGAG^{1}G^{1}G^{1}TG^{2}G^{2}G^{2}TAG^{3}G^{3}G^{3}TG^{4}G^{4}G^{4}TAA-3′

Figure 1.6. The Pu22 DNA sequence that was purchased commercially by GenScript and used in these studies. It is the same sequence that forms the structure seen in Figure 1.5.

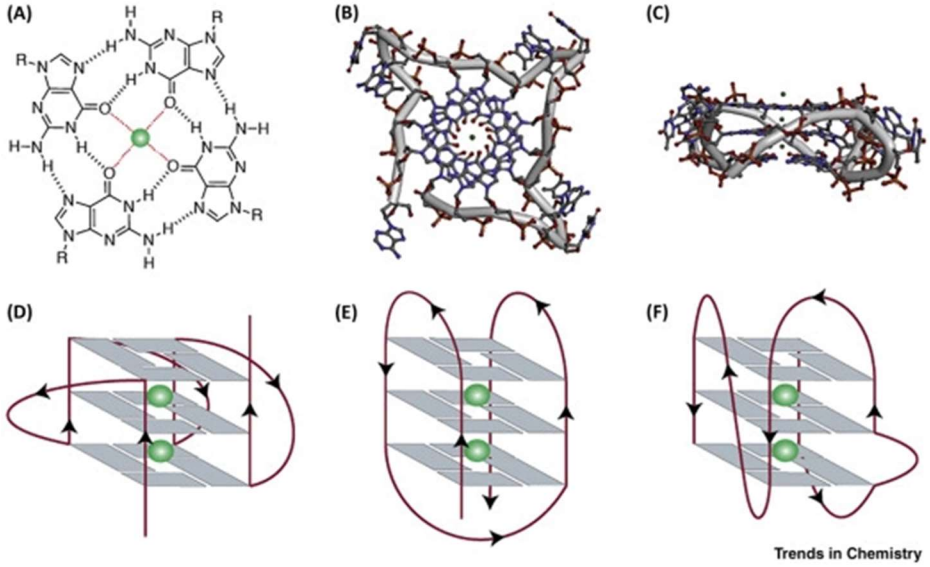

Figure 1.7. This is an example of all 3 topological types of G-quadruplex DNA. (A), (B), and (C) show the tetrad of the G-quadruplex; (D) is showing the parallel topology, (E) is showing the antiparallel topology and (F) is the hybrid topology.[28]

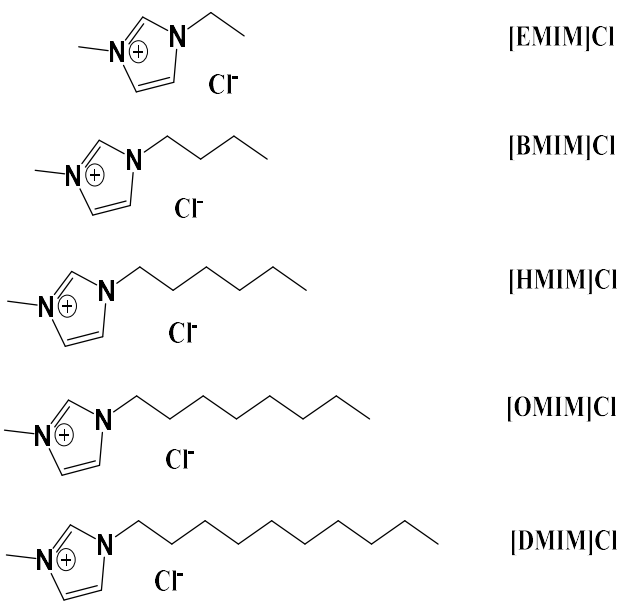

Figure 1.8. A ChemDraw figure, representing the structures of the various imidazolium chloride (ImCl) ILs. The two longest chain ImCl ILs [OMIM]Cl and [DMIM]Cl form micelles in aqueous solution.

Section 1.4 Biomolecules and ILs

There are many studies that involve protein interactions with ILs. One notable study, published in 2017 by Singh et al,[44] focused on imidazolium chloride ILs with increasing hydrophobicity. It was observed in this study that the mechanism by which the IL interacted with Cytochrome-c (Cyt-c) was with hydrophobic side chains with increasing hydrophobicity. The increasing hydrophobicity of these ILs arises from the increasing alkyl side chain length. This study was done at room temperature over a 6-month period to measure structural stability using CD spectroscopy. Structural stability was observed due to the mechanism of supporting the α-helices from hydrophobic interactions.[44]

In a separate source discussing IL interactions with Cyt-c, amino acid ionic liquids (AAILs) were used to observe stability and activity of the enzyme in the presence of AAILs.[45] This 2019 study discussed the use of both spectroscopic techniques and molecular dynamics (MD) simulations were used to identify and strengthen their understanding of AAIL interactions with Cyt-c showing structural stability and enzymatic activity in the presence of AAILs.[45] According to Sahoo et al, the CD spectra measured showed both secondary and tertiary structure. At the far-UV spectra (200-250 nm) it was observed that the secondary structure of the protein was identified through the backbone of the amino acid residues. Any changes to these spectra would indicate a change in the stability of the protein. Sahoo observed that in the far-UV range, spectra beyond 10 mM IL could not be measured as there was enhanced high tension voltage, so, IL concentrations below this value were measured. The results showed a change in the secondary structure of Cyt-c which was quantified by the CD signal at 222 nm. This

signal gave rise to α-helical content which was a result of the bond angle changing. This is an in-depth quantification of the stability of the protein based on CD signal intensity. This study concluded that AAILs where amino acids are the anion show structural stability on the protein, but not when amino acids are the cation.

There are a wide variety of studies that refer to ILs interacting with proteins.[44, 45 46 47 48 49] These studies are done on protein stability with ILs. There are various studies that have an explanation of how the IL cation or anion may play a role in the impact it has on the stabilizing of protein structures. Some studies show that ILs can stabilize protein structures.[44 45] Other studies have shown that ILs have the opposite effect.[8 12 13 48 50]

These protein-IL studies show that ILs clearly have a strong effect on proteins and more studies need to be done to determine the extent of their effects. Later in this work, proteins are used for further understanding the effects of ILs on protein tertiary structures. As mentioned before, utilizing ILs as a part of protein therapeutics and storage stability is useful in all kinds of applications.[2 3 5 9] With this in mind, the next step is to decide which ILs to study for further understanding. There is a large implication for the use of PILs, one of which being AAIL-protein interactions.

This thesis will later show results of AAILs with proteins where the amino acid (AA) is the anion. According to literature, the AAILs in which the AA is the anion should increase stability of protein structures.[8 45 48] Because AAs are the monomers of proteins in biological species, AAILs are understood to be biodegradable and less toxic than other ILs, especially choline-amino acid ILs (ChAAILs).[21 51 52] AAILs are also cost effective

as the AAs can be purchased, cheaply and in large amounts. The opposite ion to the AA in AAILs can be any other positive or negative ion, which means that AAILs can exist where the amino acid is the anion or the cation.[52] This means that AAILs can be versatile, tunable materials, and further study would be useful for a variety of applications.[2 3 5 9] Because we want to find AAILs that stabilize proteins, we chose to make AAs the anion in this study.

To understand how ILs interact with proteins, one must understand the Hofmeister effects on proteins and enzymes. The Hofmeister effects, as according to Yang, on a molecular level is far from complete even after a century of study both experimentally and computationally.[53] But the overall understanding is that "…at low salt concentrations (0-0.01 M) ions affect enzymes and proteins mainly through electrostatic forces."[54] At higher concentrations, ions have an effect with water that causes a disruption between the water molecules and the protein, causing a water-protein interaction from the ions to be a specific type of interaction. Namely, the ion starts to act like a substrate, cofactor, or inhibitor of the enzyme or protein. This could cause a slew of physical effects, like affecting the enzyme/protein activity, the stability of the molecule or protein aggregation.[53 54]

Ions can be kosmotropic or chaotropic depending on their ability to interact with water. Hofmeister effects are overall based on the understanding that changes to the bulk water structure can be affected by ions and their strength.[53] An ion can be kosmotropic when it "makes" hydrogen bonds in the water structure and an ion is chaotropic when it "breaks" hydrogen bonds in the bulk water structure.[8 53] Kosmotropic ions are typically small ions, the surface charge density is high, and the hydration is strong. Chaotropes

have a completely opposite effect to kosmotropes referring to protein-water interactions. These effects are the currently understood Hofmeister effects of kosmotropes and chaotropes on protein-water interactions.

Hofmeister kosmotropes have a very strong stabilizing effect on protein-water interactions. This means that kosmotropes can have an increase in affecting protein stability and chaotropes have the opposite effect. In the Hofmeister series, cations are observed to have a less impactful effect on protein water interactions in comparison to anions of the same charge density.[53] According to Yang, the protein-water effect that ions have in aqueous salt solutions with decreasing effects from each other are: kosmotrope-kosmotrope>kosmotrope-water>water-water>chaotrope-water>chaotrope-chaotrope.[53] For example, a kosmotropic cation and kosmotropic anion are more likely to associate (or make an ion-pair) when in water as compared to kosmotrope-water interaction because they have such high affinity for each rather than interact with water. This same interaction goes for two chaotropic ions.[53] These effects can pull away interactions of the protein surface with the water solvent that it sits in, affecting the physical effects it experiences and therefore causing an increase or decrease in stability dependent on Hofmeister effects.

ILs have been shown to sometimes follow Hofmeister series effects and sometimes not follow these effects.[54] [55] [56] [57] [58] This indicates that while the Hofmeister series is a good model to follow for understanding some IL effects on proteins, it cannot completely explain protein-IL interactions. From the understanding of Hofmeister effects, it can be understood that an IL made up of a chaotropic cation and a kosmotropic anion would be the ideal IL composition for protein-IL stabilization effects and to maintain

activity.[53] Even knowing this, there are still other effects like hydrophobicity and polarizability that can explain IL-protein interactions.

Kosmotropic and chaotropic effects are also known to be related to viscosity of ILs. This can be seen in the Jones Dole equation.[53] The B value in the Jones Dole equation is used to quantify viscosity and can indicate whether a cation or anion is kosmotropic or chaotropic. With the understanding that IL cations and anions could be either kosmotropic or chaotropic, can tell us about the kind of ions to use to tune ideal ILs.[53]

It is understood that the D-form of amino acids are typically more kosmotropic ions, but that understanding is very broadly understood when it comes to amino acids.[53] Overall, this knowledge is necessary for understanding how AAILs fit into the narrative of protein structure stabilization.

To round out our discussion of ILs with biological macromolecules, there is insight to lead to further study of ILs with protein and G-quadruplex DNA/RNA. There is indication that ILs have an effect on the structure and in turn, thermal stability of the G-quadruplex.[35] [59] There are many kinds of ILs that have differing effects on proteins and DNA/RNA structures. ILs, as mentioned before, are molten liquid salts at room temperature. Unlike other salts, they rarely form a completely solid form and instead supercool when falling below the freezing point and undergo a glass transition.[60] Depending on the cation or anion present there can be a completely different observed effect. For example, imidazolium based ILs can be tuned by increasing the length of the alkyl chain and therefore increase hydrophobicity. This attribute of ILs allows them to be

useful tunable substances for a collection of physical interactions. ILs are a suitable candidate for our study on both proteins and DNA as described later in this work. ILs have a broad potential for the future in pharmaceuticals, catalysis, or biofuels.[18 51 61 62] With this in mind, understanding fundamental physicochemical properties of ILs on different biological molecules is important for understanding their usefulness in therapeutics in the future.

Section 1.5 Amino Acid Ionic Liquids (AAILs)

Recently, amino acid ionic liquids (AAILs) have been used in pharmaceuticals and other "green chemistry" as they are biodegradable.[51 52 63] Amino acids (AAs) are the building blocks for proteins and therefore have a large implication to be used as safe excipients in formulations of pharmaceuticals. They also have many implications for interactions with proteins, so studies on protein therapies or industrial applications of proteins in environmental applications show promise for new studies.[4 19 44 45 61 62]

AAILs are biocompatible as amino acids are monomers of proteins in the human body. These AAILs have shown effects on biological systems.[15 51 52] With this in mind, this means that AAILs are a perfect target for study and useful, tunable material for testing biological molecules. As mentioned previously, there are many studies in which AAILs have shown promise for development as solvents or use in stabilization of biological molecules.[7 15 64 65] For this reason, we have chosen AAILs for the study involving protein interactions. Imidazolium chloride ILs were also utilized to test hydrophobic interactions on G-quadruplex DNA/RNA structures.

Section 1.6 Choline Based AAILs

AAILs have been synthesized and studied as far back as 2005 by Fukumoto and his group.[66] The amino acids used were of the 20 essential amino acids and the cation in this study was 1-ethyl-3-methylimidazolium (EMIM).[66] Imidazolium based ILs have been around for decades as well and an alternative with less toxicity would be a wonderful target of study.[52] Using a molecule that is already present in biological systems may lead to a decrease toxicity.[22] It was discovered that choline is a biocompatible IL component as it is a molecule that is present in biological systems.[22 67] The structures of choline and some of the utilized amino acids in this study can be seen in Figure 1.9. There are various studies indicative of the physicochemical properties of some choline-amino acid ILs (ChAAILs) which have identified properties like decomposition temperature and viscosity.[21 68] The effect of these ILs on biological systems has some gaps left to be filled.[23 65 69 70] Some understanding of the toxicity of AAILs has been researched and outlined.[15 65 69] The studies available for understanding how AAILs are affecting biological systems have gaps, and this study can help improve the knowledge and understanding of ILs to help fill in that gap.

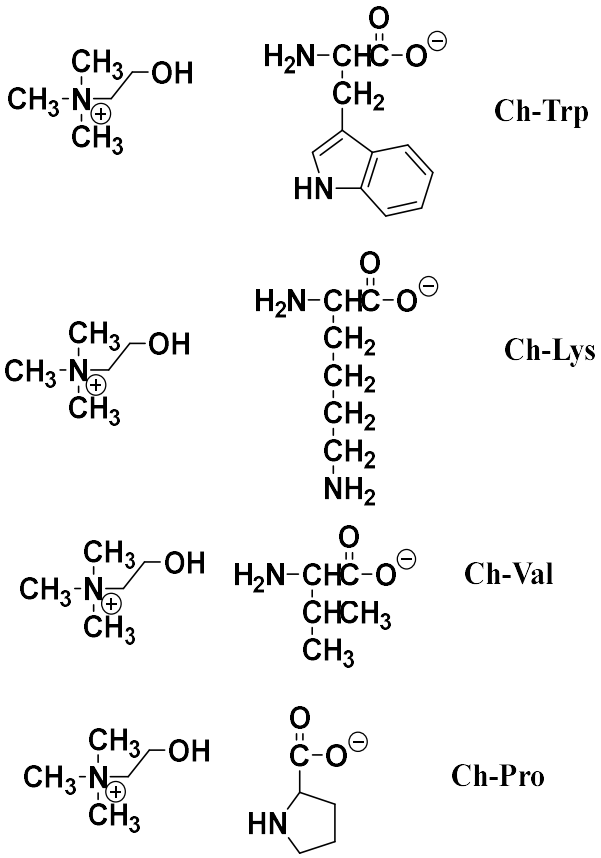

Figure 1.9. ChemDraw choline AAIL structures. This figure shows the choline cation on the left side of the figure, and some of the amino acid anions that were paired with the choline cations.

Section 1.7 TMG Based AAILs

The next kind of AAIL utilized in these studies is that with a different cation base. The cation in this case is 1,1,3,3-tetramethylguanidine (TMG) which is a molecule with a guanidine base and 4 methyl groups attached at the 1st and 3rd carbons around the guanidine base. This molecule allows for in-house synthesis of ILs as it is a commercially available substance. It has many nitrogen atoms in the structure which provides the potential of being a cation with amino acid anions as an AAIL. TMG is a molecule that is environmentally friendly and easy to use for synthesis.[17] The TMG molecule has promise for future biotechnology and little study has been done on TMGAAILs. This study is hoping to provide more information of TMGAAIL physicochemical effects. Some of the studies with TMG based ILs are mentioned here.[11 13 17 50 71 72] Because it is more environmentally friendly, this allows for more use in agriculture or other biotechnology as study has been done to show that TMG cation based ILs are biodegradable compared to other ILs.[72] The structure of TMG and some of the 20 essential amino acids can be seen below in Figure 1.10.

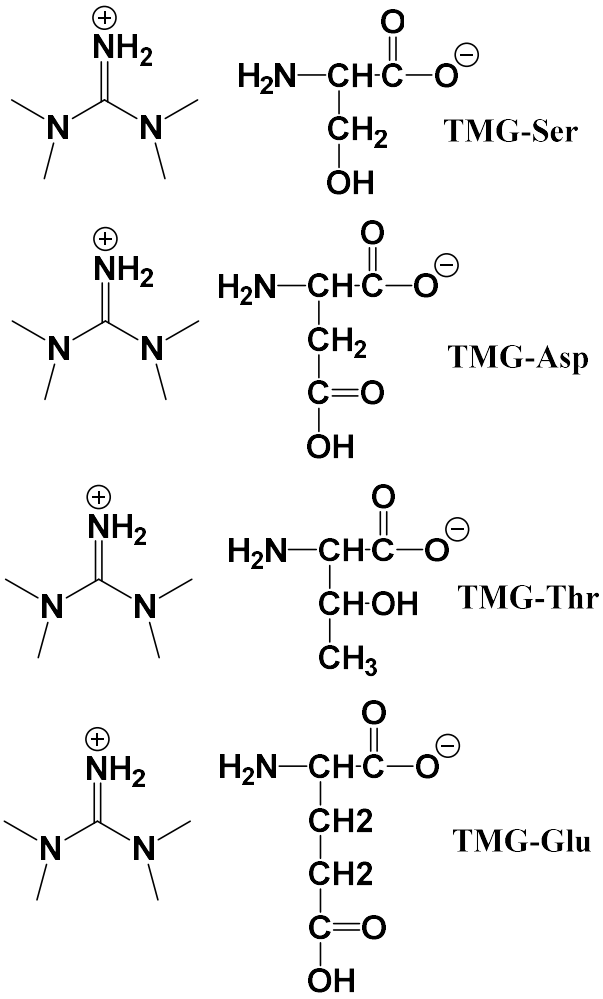

Figure 1.10. The figure shows a ChemDraw of TMG (left side) and some of the many amino acids (right side) tested in the studies below.

Section 2 Experimental Techniques

Section 2.1 Synthesis of ILs

Section 2.1.1 Synthesis of ChAAILs. The technique for synthesizing the ChAAILs was adapted from a paper on cholinium-amino acid based ILs by De Santis et al.[56] Amino acid was obtained commercially in its L chiral isomer form. This amino acid is weighed out for a 1:1 mole ratio of amino acid to choline respectively. Then an extra ~10% excess is added and the solid is dissolved in DI water and stirred for about 20-30 minutes. Then, the volume of choline hydroxide was added dropwise until it is all stirred in completely. During this time, the solution is kept in an ice bath around 0-5^{o}C overnight. This solution was then evaporated under vacuum until all water was removed. The sample was mixed with 20 mL of a 9:1 ratio of acetonitrile and methanol and allowed to stir for 20-30 minutes to precipitate the excess amino acid that did not react. This sample was then subjected to vacuum filtration to separate the precipitated amino acid from the IL and the solvent. This separated solution was then poured into another clean and dry round bottom flask and the solvent was evaporated under vacuum until all solvent was removed. After the solvent is removed, we then added a step of using charcoal to completely decolorize every AAIL that was used in these studies. This was to make sure that no color was present to absorb the light in the region that we detect the biological sample.[73] 10 mL of DI water, and about 1.5 g of activated charcoal were added to the AAIL sample and mixed for about 45 minutes. After stirring, the charcoal and AAIL solution was poured through a vacuum filter once again and from this point, all charcoal was removed, and we were left with our AAIL dissolved in water. The water

was removed by evaporation under vacuum. These AAILs were then analyzed using FT-IR and compared to known IR spectra of ChAAILs.

Section 2.1.2 Synthesis of TMGAAILs. TMGAAIL synthesis and purification was adapted from previous works.[11 50 74] TMG and amino acid were mixed in a 1:1 mole ratio in water under nitrogen purging during stirring. After sufficient stirring, water was evaporated under vacuum. Then, 10 mL of DI water was added to the IL along with 1.5 g of activated charcoal and allowed to stir for 45 minutes. Next, the sample was put through vacuum filtration and the water from the sample evaporated under vacuum as well.

Section 2.2 Preparing Proteins for Study

Both azurin and mCherry have a very specific synthesis and purification procedure that has a unique way of isolating the desired protein. While both proteins have specific techniques for isolating the desired protein, some steps are similar. Azurin was purchased through Genscript (Piscataway, NJ) utilizing the plasmid (PDB ID "1AZU") from *Pseudomonas aeruginosa* and incorporated into kanamycin resistant *E. coli* for easy growth and expression. For mCherry (PDB ID "2H5Q"), the plasmid pet28b was purchased from GenScript (Piscataway, NJ) and incorporated similarly to azurin and the *E. coli* was utilized for overexpression.

The procedure for purifying azurin has been well studied and was adapted from past sources.[12 13] The kanamycin-resistant *E. coli* was streaked on an LB Agar plate containing 10 μg/mL of kanamycin and allowed to grow overnight in an incubator kept at 37°C. From this plate, a single colony was chosen, assuming that this colony was

replicated from a singular bacterium. This colony was added into a 3 mL solution of LB broth with 80 μg/mL $MgSO_4$, 1 μg/mL $CuSO_4$, and 10 μg/mL kanamycin and grew overnight at 37°C. This culture was poured into a large 1 L broth of the same nutrients kept at 37°C and shaking at 170 rpm. This broth of *E. coli* was allowed to reach exponential growth phase when the OD_{600} more than doubled from the previous measurement. At this point, a 0.1 M solution of Isopropyl ß-D-1-thiogalactopyranoside (IPTG, Alfa Aesar) was mixed with DI water and added to the 1 L broth to reach a final concentration of 0.1 mM IPTG.

The next step occurs at least six hours after adding the IPTG to induce expression. The 1 L broth was then poured into centrifuge bottles and placed in a *Beckman Coulter JLA-16.250 rotor* which was then placed into a *Beckman Coulter Avanti JXN-26 centrifuge* and spun at 11,000 rpm for 20 minutes. After the centrifugation, the supernatant was decanted, and the pellet was saved. This would then be centrifuged on a different benchtop centrifuge, a *Beckman Coulter Allegra X-14R centrifuge*, and the pellet was saved and kept in a -80°C freezer. Up until this point, the same procedure was used for mCherry.[12]

Section 2.3 Azurin Protein Purification

The next day, the saved pellet of *E. coli* cells was taken out of the freezer and a lysis buffer (pH 8.1, Tris base 0.01 M, 20% sucrose and 1 mM EDTA) was added to the pellet and vortexed. Once ready to start lysis, 12 mg of refrigerated lysozyme was added to the solution to aid in the breakdown of the cell membrane. After vortexing, the solution was placed in an ice bath and sonicated. This sonication occurred for 2 minutes,

15 seconds on and 15 seconds off at 40% amplification. The tip used has around 46 amplitudes at 40% amplification. Next, this solution is centrifuged in a *Sorvall SS-34 rotor* which was then secured in a *Sorvall RC5B Plus centrifuge* and centrifuged at 12,000 rpm for 20 minutes. Afterwards, the supernatant was kept, and the pellet was discarded.

Next, this solution was mixed with a buffer containing 0.5 M ammonium acetate and pH adjusted to 4.1. After letting this mixture sit for 30 minutes, while stirring occasionally, the solution was centrifuged once again at 10,000 rpm for 20 minutes. After the centrifugation process, the pellet was discarded, and the supernatant was kept. This solution contained the azurin protein and needed to be further purified through column chromatography.

The separation technique used in the purification of azurin was ion exchange chromatography, specifically cation exchange. The cation exchange separation utilized pH change to separate the protein from the stationary phase. This column utilized CM-sephadex fast flow resin (GE Healthcare) as the matrix for the stationary phase. This stationary phase is a weak cation exchange resin. The mobile phase used to equilibrate the column was a 0.05 M ammonium acetate buffer at pH 4.1. After column equilibration, the centrifuged supernatant from the previous step was added to the top of the column. The mobile phase was changed to a second buffer to elute the protein, 0.05 M Ammonium acetate buffer with pH 5.1. In the fractions collected from this first run, there was 10 µL of 0.5 M $CuCl_2$ then each fraction was tested for the presence of azurin protein by saving fractions with the greatest absorbance at 680 nm. After column re-equilibration, the saved protein fractions were added to the column and a pH gradient

elution procedure was used. The first buffer used was 0.05 M ammonium acetate pH 4.1, and the final buffer was, 0.05 M ammonium acetate pH 9.1, to elute in a gradient from pH 4.1 to 9.1. The bluest fractions were then saved, dialyzed, and lyophilized.

Section 2.4 mCherry Protein Purification

A similar protein purification technique came from a previous study in our group.[11] After *E. coli* cell growth and extraction, 15 mL of a lysis buffer (5 mM PBS (phosphate buffer saline) with 10 mM NaCl and 5 mM EDTA) was added to the cell pellet. This solution was resuspended by vortexing until homogenous. After letting the sample sit for 5-10 minutes, the sample was placed in an ice bath and sonicated. The mCherry sonication was 2 minutes time, 30 seconds on, 30 seconds off at 40% amplification repeated 10 times. Following this step, the sample was centrifuged at 17,000 rpm for 15 minutes, the pellet in the centrifuged sample was discarded and the supernatant was saved.

The first utilized separation technique was ammonium sulfate precipitation. The sample needed to be brought up to a concentration of 50% ammonium sulfate, and to do this, the concentration needed to be calculated using the EnCor Biotechnology website. The value of mass needed was then weighed out and added slowly to the sample while stirring over the course of an hour at room temperature. After stirring, the sample was centrifuged in the same *Sorvall RC5B Plus centrifuge* at 17,000 rpm for 20 minutes. The pellet was then discarded, and the supernatant was saved. To precipitate out mCherry protein, the sample was brought to 65% ammonium sulfate concentration over the course of another hour while stirring to ensure complete precipitation. This sample then needed

to be centrifuged as well in the same centrifuge at 17,000 rpm for 20 minutes. The pellet was saved from the sample, and the supernatant was tossed out as waste. The pellet was resuspended using a 10 mM PBS buffer. The sample was transferred to dialysis snakeskin tubing with a MWCO of 10,000 (ThermoFisher). The tubing with the sample was placed into a large 4 L bucket of dialysis buffer, containing 5 mM PBS at pH 7 with 10 mL of Tween 20 (Amresco) added to reduce the protein from sticking to the snakeskin tubing. This dialysis was allowed to stir slowly overnight for a maximum of 12 hours.

The dialysis bag was taken out of the 4 L bucket of dialysis buffer and then transferred into a centrifuge tube and centrifuged for about 10 mins at 4,200 rpm in the *Beckman Coulter Allegra X-14R centrifuge*. The pellet was tossed in the waste and the supernatant is saved and added to an ion exchange chromatography column. The stationary phase utilized in this procedure is a Q-sephadex matrix (GE Healthcare). The mobile phase that was used to equilibrate this column was a low NaCl PBS buffer with 20 mM phosphate pH 7 and 10 mM NaCl. The resin is washed with this buffer for 3 column volumes. The mCherry was eluted using a mobile phase gradient hopper and a pump. The first buffer was a low salt buffer (10 mM phosphate, pH 7 and 10 mM NaCl) previously used to equilibrate the resin. The second buffer of high salt (10 mM phosphate, pH 7 and 100 mM NaCl) was added to fill the same volume of low salt buffer added. This technique was to elute the mCherry over a salt concentration gradient. Throughout this run, 2 mL fractions were collected sequentially.

The 10 most purple samples were saved and tested utilizing SDS-PAGE. The SDS sample buffer contained 66 mM Tris-HCl, pH 6.8, 26% (w/v) glycerol, 2% SDS, 0.01% bromophenol blue and 10% β-mercaptoethanol which needs to be added just

before starting the experiment. The tank buffer for running the gel was 0.025 M Tris, 0.192 Glycine, 0.1% SDS and pH 8.3 for running the SDS-PAGE at 190 V for about 90 minutes. The gel was then removed from its casing and placed into a holder from a *GenScript eStain L1 Protein Staining System*. This staining system comes prepped ready to run Coomassie staining solution and de-staining solution through the gel in a matter of 10 minutes. The fraction samples with the most mCherry protein were saved. These samples were placed into snakeskin dialysis tubing with MWCO of 10,000 Da (Thermofisher). The same 4 L dialysis buffer was made again and allowed to stir overnight slowly for the maximum 12 hours to dialyze. The final step is to freeze the sample in liquid N_2 and place it on a *LabConco FreeZone 25 Plus* lyophilizer to obtain solid mCherry protein for thermal stability studies.

Section 2.5 G-quadruplex DNA/RNA Preparation

The ILs used in these experiments were 1-decyl-3-methylimidazolium chloride ([DMIM]Cl, Tokyo Chemical Industry, 96%), 1-methyl-3-n-octylimidazolium chloride ([OMIM]Cl, Alfa Aesar, 97%), 1-n-hexyl-3-methylimidazolium chloride ([HMIM]Cl, Alfa Aesar, 98%), 1-butyl-3-methylimidazolium chloride ([BMIM]Cl, Tokyo Chemical Industry, 98%), and 1-ethyl-3-methylimidazolium chloride ([EMIM]Cl, Aldrich, 98%). These IL structures can be seen in Figure 1.8. The buffer used for all experiments was 10 mM Tris buffer pH 7.5 with 0.1 mM ethylenediaminetetraacetic acid (EDTA). This buffer, and most solutions used throughout DNA/RNA experiments, was kept free of K^+ and Na^+ unless stated otherwise. The correct pH was achieved by optimizing amounts of Tris and TrisHCl. In some tests, KCl was added to the buffer at a concentration of 100 mM.

Lyophilized G-quadruplex DNA (sequence 5'-TGAG^{1}G^{1}G^{1}TG^{2}G^{2}G^{2}TAG^{3}G^{3}G^{3}TG^{4}G^{4}G^{4}TAA-3') was obtained from *GenScript* (Piscataway, NJ). A 50 mM stock solution was prepared in the K^+-free buffer and subjected to an annealing procedure[75] in which the solution was heated to 95°C for 5 minutes then allowed to cool to room temperature on the bench and stored overnight at 4°C. The DNA concentration in all final solutions was 5 mM. All solutions, except the G-quadruplex DNA stock, were prepared fresh at room temperature about 1 hour prior to measurement. These same techniques are applicable to G-quadruplex RNA prepared for thermal unfolding experiments. Some samples were made with K^+ by adding 100 mM KCl to the buffer used.

Section 3 Spectroscopy

In this work, there are many techniques utilized to analyze the effects of ILs on biological systems outlined herein. Proteins are typically concentrated enough for techniques like CD spectroscopy and fluorescence spectroscopy for thermal stability studies. DNA/RNA thermal stability studies can be analyzed with CD spectroscopy as well.

Circular dichroism (CD) spectroscopy was performed with a *JASCO J-1500 CD Spectrometer* that utilizes a Peltier-based heating device and a *Koolance EXOS Liquid Cooling System* for temperature control. Samples were placed in a 1 mM pathlength quartz cuvette and capped to prevent water evaporation.

Fluorescence spectroscopy was utilized for collecting thermal unfolding assays of azurin protein. The spectrofluorometer used is a *Horiba FluoroMax* with thermal control

unit *Quantum NorthWest TC 1 Temperature Controller* and a *Koolance EXT-440 Liquid Cooling System* to cool or heat the cuvette holder. Samples were then placed into a 3 mm path length fluorescence quartz cuvette and capped to prevent water evaporation.

CD spectroscopy is a useful technique for a deeper understanding of chiral molecules. It is understood that amino acids are chiral molecules which make proteins the perfect target of study with CD spectroscopy techniques.[76] CD spectroscopy helps us to analyze chiral molecules by sending polarized light through the sample. If the chiral molecule in the sample is more right-handed than left-handed, then the spectrum will exhibit a negative peak in the peptide bond absorbance region.[76] If the signal is more left-handed than right-handed, then the CD signal will exhibit a more positive than negative peak.[76] This comes from the circular polarized light being made into an elliptical pattern which is specific only to chiral molecules bending the light.[76] This bending of light in one direction more than another is known as dichroism. CD Spectroscopy, in our case, is measured in units of mdeg. This technique is useful for chiral molecules like proteins and G-quadruplex DNA. This will be helpful for identifying the molecule and give rise to interpretation of the secondary and tertiary structures being interrupted in any way.

The next spectroscopic method utilized was fluorescence, which is a particularly sensitive technique. While fluorescence is not always used for protein stability studies, it is very useful for the study of the protein azurin which will be discussed in greater detail in this study. Azurin has a single tryptophan residue buried in the center of the protein and, when excited at 285 nm, the tryptophan residue has an emission at 308 nm. This can be seen in Figure 1.2 where the peak is in the region of 308 nm when folded. When the protein is unfolded and excited at 285 nm, the tryptophan residue is exposed to the

surrounding water and solvation effects give rise to emission energy at 355 nm. This altered fluorescence from the single tryptophan residue can help us identify folded versus unfolded azurin protein so that thermal stability can be quantified.

Fluorescence works through sending a wave of energy in the form of a photon to the sample at a very specific wavelength. The wavelength chosen is based on the excitation of the highest occupied molecular orbital (HOMO) of the fluorophore. When the photon of the excitation wavelength hits the sample, it excites the electron in the HOMO and then sits in the lowest unoccupied molecular orbital (LUMO) briefly and the energy released as the electron moves back to the HOMO is the emission fluorescence signal.[77] [78] This emission signal is very sensitive and gives rise to the shape of the graph of fluorescence from the fluorophore. For example, in Figure 1.2, the emission from 295 nm to 450 nm of azurin in aqueous solution is shown at 25 ^{o}C and 85 ^{o}C.

Chapter 2

Fundamental Thermal Destabilization Studies on the Protein Azurin With Both Choline and TMG Amino Acid Ionic Liquids (AAILs)

Section 1 Introduction

It is well known in the scientific community that proteins are an important therapeutic and a model substance for improving disease treatment and novel drug development.[2 3] Specifically, there are a wide variety of protein secondary and tertiary structures that play roles in both its function and stability. Azurin is an optimal choice of model protein because of ease of availability and the mixed tertiary structure. The azurin protein contains both α-helices and β-sheets which makes the protein an ideal model for fundamental IL studies.[12] As mentioned previously, AAILs have seen some study on proteins.[11 45 49 50] And there are vastly more protein-IL studies that involve different IL cation-anion structures that show varying conclusions.[44 46 74 79 80 81] This thesis seeks to further improve the knowledge on AAILs and provide an organizational, or fundamental difference between different AA structures and relate them to protein-IL thermal stability effects. The simplest way this can be done is organizing by AA side chain structure and analyzing for an observable pattern. It is known that there are a variety of interactions that proteins experience to cause thermal unfolding. AA residues have stronger or weaker effects on stabilizing the protein, internally or externally, depending on the temperature of the environment. Therefore, the effect that external AAILs have on protein thermal stability has little understanding, and much of what can provide insight in this study will be based on Hoffmeister effects and intermolecular forces from AAILs on protein-water surface interactions.[55 82 83]

Section 2 Experimental Data

The thermal stability studies outlined herein were completed by using fluorescence to observe structural changes in the azurin as a function of temperature. Solutions were made with 1 mg/mL of azurin and 0.5 M AAIL in DI water. These samples were placed in a small 125 μL cuvette and placed into a Horiba Fluoromax for obtaining the fluorescence spectra. The procedure is as follows:the excitations wavelength was set to 285 nm, and the emission spectra measured 295-450 nm. The temperature was set to 25 ^{o}C to start, then the temperature is increased by ~5 ^{o}C until unfolding is reached. Embedded between the β-sheet structures in azurin, there is exactly one tryptophan residue in the azurin protein. This can be seen in Figure 1.1 as the red ball. When the azurin protein is folded in its natural state, the tryptophan residue will emit at a wavelength of 308 nm once excited at 285 nm. This intense peak at 308 nm will shift to the red at 355 nm when unfolded, or denatured, and exposed to the solvation effects of water. An example of folded and unfolded azurin protein can be seen in the previous chapter in Figure 1.2. Because fluorescence is a very sensitive technique, there is an obvious shift or change to the spectra, even with as little as 1 mg/mL of azurin protein present in solution.

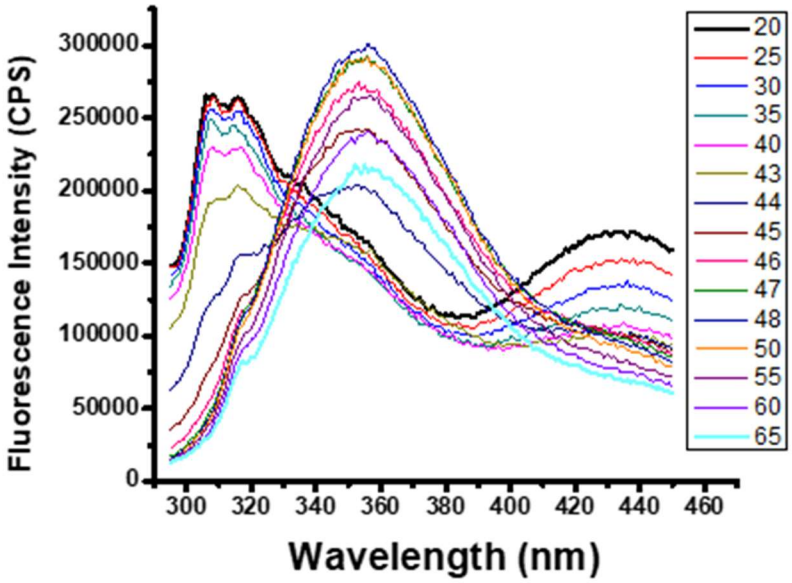

Figure 2.1. This is a Sample of the Fluorescence Spectra of 1 mg/mL of Azurin with 0.5 M TMGSer. This shows spectra measured across increments of 5 °C until the azurin unfolds. Each spectrum is excited at 285 nm and measured 295-450 nm.

$$F_u = \frac{\left(I_{355}/I_{308}\right) - \left(I_{355}/I_{308}\right)_{folded}}{\left(I_{355}/I_{308}\right)_{unfolded} - \left(I_{355}/I_{308}\right)_{folded}}$$

Figure 2.2. This is the equation used for calculating a ratio of the intensity at 355 nm divided by the intensity at 308 nm to get an unfolding fitting curve based on the folded and unfolded state approximation.

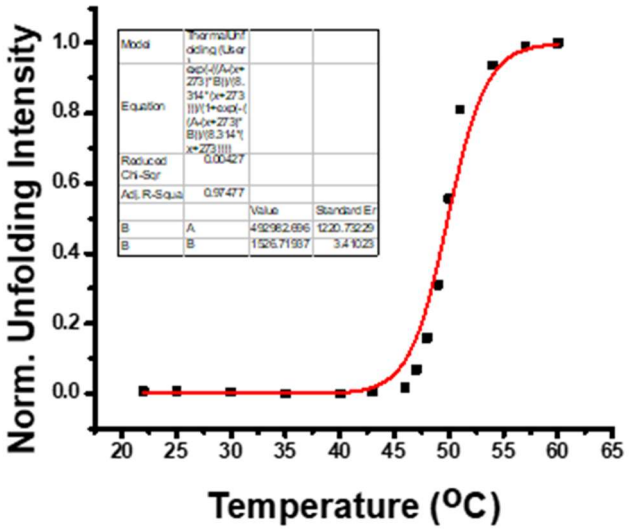

Figure 2.3. A sample unfolding curve for 0.5 M TMGSer. Each temperature measurement can be seen outlined on the x-axis and the y-axis shows normalized fluorescence intensity from the previous analysis outlined in Figure 2.2.

$$F_u = \frac{e^{\frac{-\left(\Delta H^{\circ}_{unf} - (T+273)\Delta S^{\circ}_{unf}\right)}{R(T+273)}}}{\left(1+e^{\frac{-\left(\Delta H^{\circ}_{unf} - (T+273)\Delta S^{\circ}_{unf}\right)}{R(T+273)}}\right)}$$

Figure 2.4. The equation used to fit a line to the unfolding curve shown in Figure 2.3. This equation relates temperature to unfolded fraction of protein, which can provide us with ΔH_{unf} and ΔS_{unf}.

An example of a full experiment with all spectra can be seen in Figure 2.1. This experiment was done with 0.5 M TMGSer and 1 mg/mL azurin and it was conducted with increasing temperature in ~5 ^{o}C increments past protein unfolding. With these spectra we can utilize the equation in Figure 2.2 to provide a ratio of folded protein indicated by 308 nm, and the unfolded azurin protein at 355 nm. As the 308 nm intensity decreases, the 355 nm intensity peak increases simultaneously in most cases, and this will provide an unfolding curve data set of the ratio of fluorescence intensities as a function of increasing temperature. These data points can be plotted and normalized as seen in Figure 2.3 with a line fitted to the data points as well. This fitting function can be seen as the equation in Figure 2.4 relating temperature (x-value) to fraction unfolded protein (y-value). This fitting equation can provide information such as $\Delta H_{unfolding}$ (ΔH_{unf}) and $\Delta S_{unfolding}$ (ΔS_{unf}) which is useful for identifying how the ILs affect the thermodynamics of the protein's thermal stability. In Figure 2.5, one can see the unfolding curves of the 0.5 M TMGAAILs in the presence of azurin. The y-axis is normalized unfolded fraction, which translates to 1 being the unfolded protein and 0 being the folded protein as can be interpreted by our analysis forming an unfolding curve, derived from the equation in Figure 2.2. The inflection point, where the unfolding curve is halfway on the y axis, indicates the melting temperature (T_m) of the protein in the presence of the AAIL. For example, the inflection point of 0.5 M TMGVal is around 42^{o}C. A similar figure was generated from the 0.5 M ChAAILs with azurin which can be seen in Figure 2.6. This figure can be analyzed in a similar way, observing the inflection point of each unfolding curve as the T_m of each AAIL. The next data set to observe is the graph of melting temperatures. Here, in Figure 2.7, you can see the T_m of all 0.5 M TMGAAILs on azurin

organized by decreasing destabilization. Similar in fashion to the previous figure, one can see another summary figure of all T_m values for 0.5 M ChAAILs with azurin in Figure 2.8.

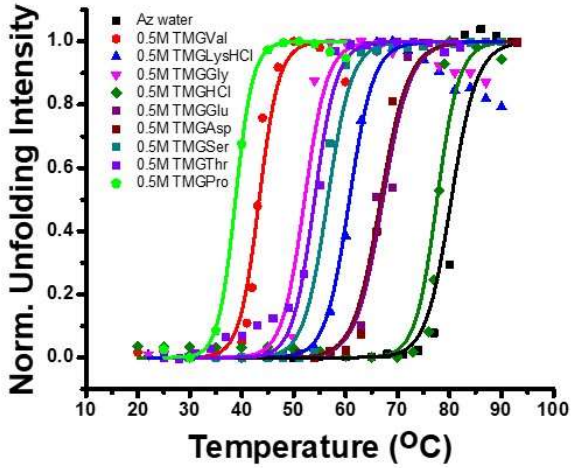

Figure 2.5. A summary figure of 0.5 M TMGAAILs with 1 mg/mL azurin thermal unfolding curves. On the y-axis, 0 indicates folded protein and closer to 1 indicates unfolded protein.

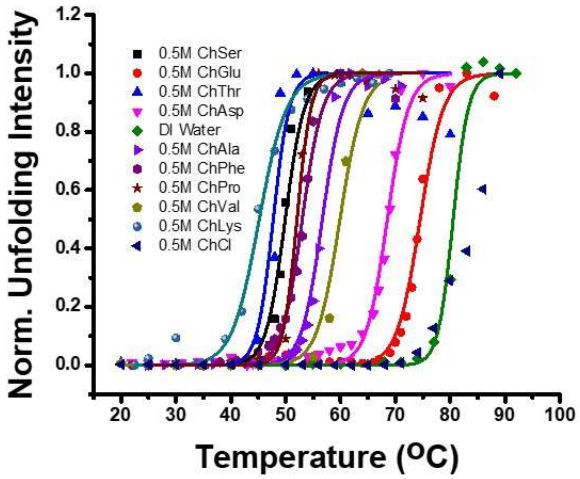

Figure 2.6. This is a summary figure of all 0.5 M ChAAILs tested with 1 mg/mL azurin thermal unfolding curves. Any shift to the right, from the control sample, indicating an increase of melting temperature (at half max) would mean stabilizing the protein.

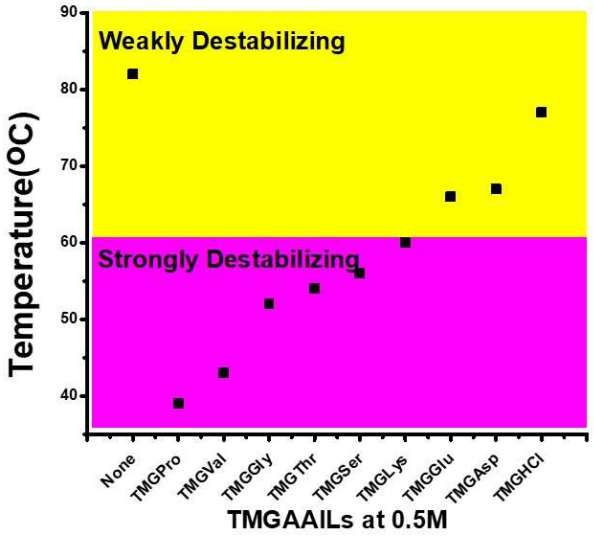

Figure 2.7. This is a figure showing the T_m values for each 0.5 M TMGAAIL on azurin. These values are organized by decreasing destabilization.

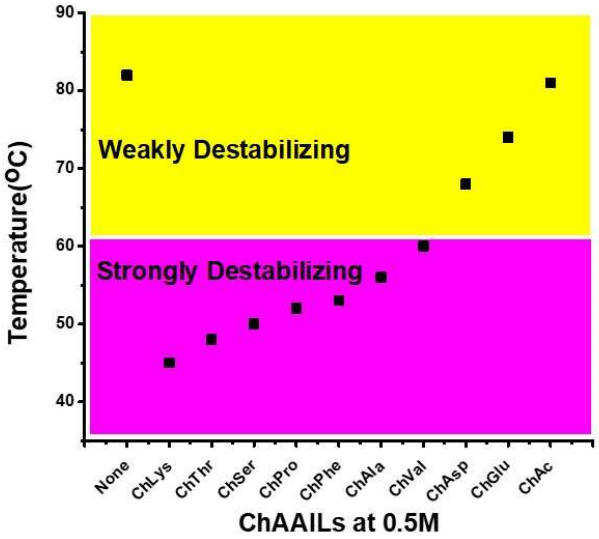

Figure 2.8. This shows the T_m values of all 0.5 M ChAAILs tested on azurin organized by decreasing destabilization.

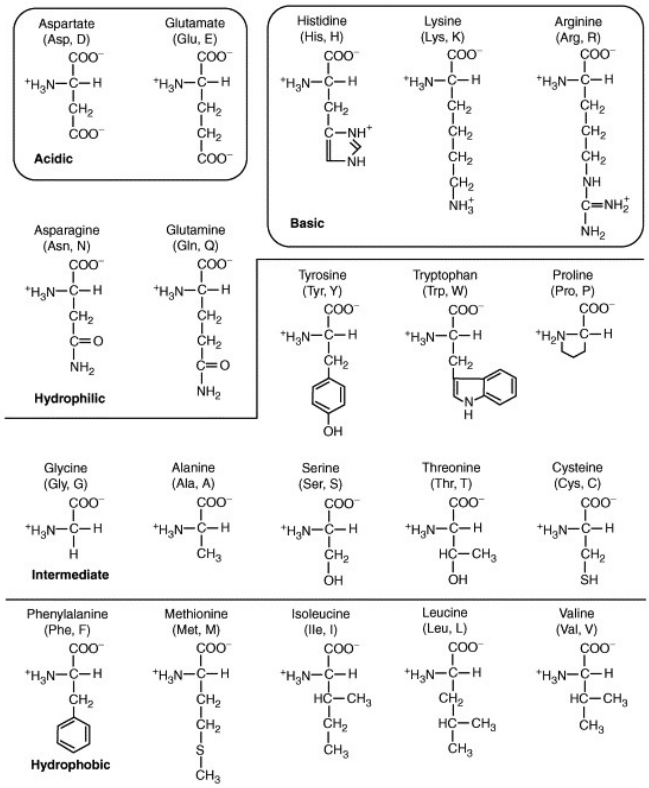

Figure 2.9. These are the 20 essential amino acid (AA) structures organized by similar side chain properties. Basic lead to positively charged side chains, acidic lead to negatively charged side chains.

Section 3 Discussion

The data provided can be analyzed and interpreted in many ways. But the main objective interpretation comes from Figures 2.5 and 2.6. In these figures, any unfolding curve with a shifted inflection point with respect to the control sample (DI water) can indicate thermal stabilization or destabilization. Any shift of the inflection point to the left (lower temperature) of the initial control sample of azurin would indicate a thermal destabilization of the azurin. In both Figures 2.5 and 2.6, all TMGAAILs and ChAAILs have an inflection point shifted to the left. This shift to the left indicates a decrease in the T_m and therefore a thermal destabilization of the azurin protein in the presence of 0.5 M TMGAAILs or 0.5 M ChAAILs. One can try to identify a pattern in the destabilization effect of the AAILs based on the structure of the side chain of the AA in AAILs and their properties. These properties can be seen in Figure 2.9 with the common side chain structures and properties of the 20 essential AAs. It is well known that hydrophobic effects are the strongest and most impactful for causing protein folding.[82] But when it comes to protein stability and protein unfolding, the strongest effects that scientists come to agree affect protein unfolding are H-bond interactions and other intermolecular forces.[45, 54, 83 84 85]

As mentioned previously by Sahoo et al, AAILs have been seen to show increasing protein stability when AAs are the anion, not the cation.[45] Regarding the data provided above, both the TMGAAIL and ChAAILs, where the AA is the anion, indicate that there is a decrease in the thermal stabilization of the azurin protein. The AAs being the anion can indicate that these AAILs *should* further stabilize the azurin protein in reference to Sahoo, Miller and Patel's works.[8 45 48] But, as seen in this study, there is an

opposite indication, specifically with the mixed structure protein azurin. This is another indication, as mentioned by Pucci, that there are somewhat confusing and contradictory results on physicochemical effects that impact protein unfolding the most.[58 79 82 86] One can see in Figure 2.10 the organization of the T_m values by AA side chain property. In Figure 2.10A, the T_m values come from the 0.5 M TMGAAILs and in Figure 2.10B, the T_m values come from the 0.5 M ChAAILs. For further understanding, choline is more biocompatible than TMG, and there is some small difference of AAILs with choline vs TMG. Choline is a commonly found molecule in human biology. It is in many foods and very easily consumed so its usefulness as a cation in AAILs has biocompatibility.[67] In a review about the essentiality of choline, there is discussion of choline being used for synthesis of essential biomolecules like phosphatidylcholine (phospholipid for membrane synthesis) and a precursor for acetylcholine (common neurotransmitter).[67] Choline has yet to be identified as an essential nutrient as it can be synthesized in the human body through the sequential methylation of phosphatidylethanolamine.[67]

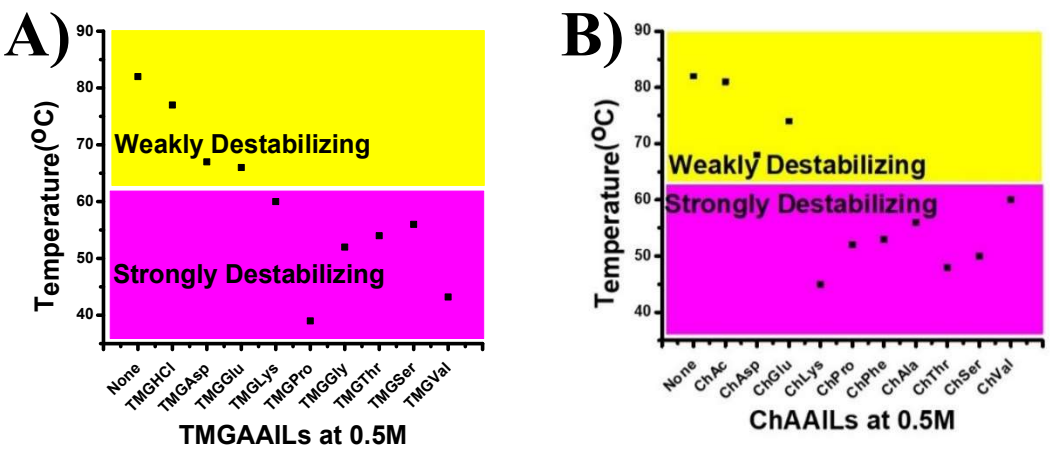

Figure 2.10. This figure shows all AAIL melting temperatures organized by amino acid side chain property in which there are two separate graphs A) including all 0.5 M TMGAAILs and B) all 0.5 M ChAAILs.

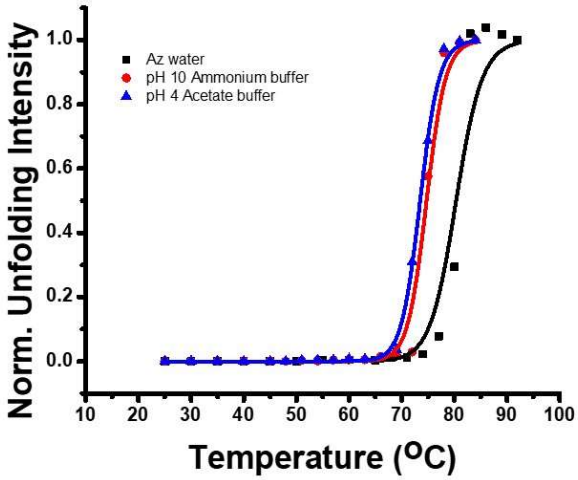

Figure 2.11. These are normalized unfolding curve figures of control pH experiments run in a range from 4 to 10 of 20 mM ammonium acetate.

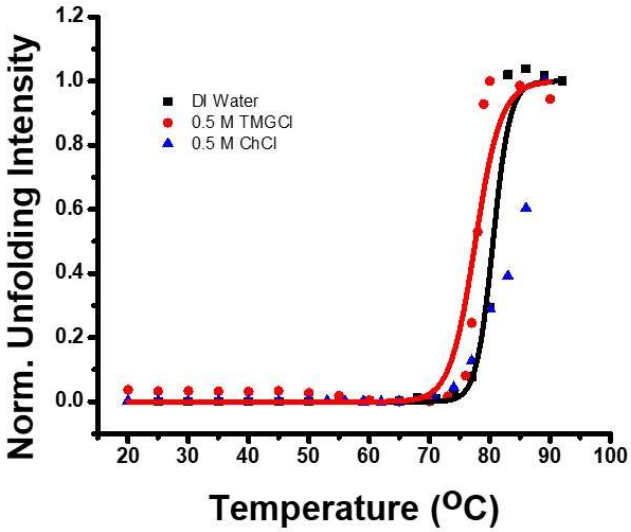

Figure 2.12. Control unfolding experiments with azurin, comparing TMG^+ and Ch^+ cations as ILs with Cl^-.

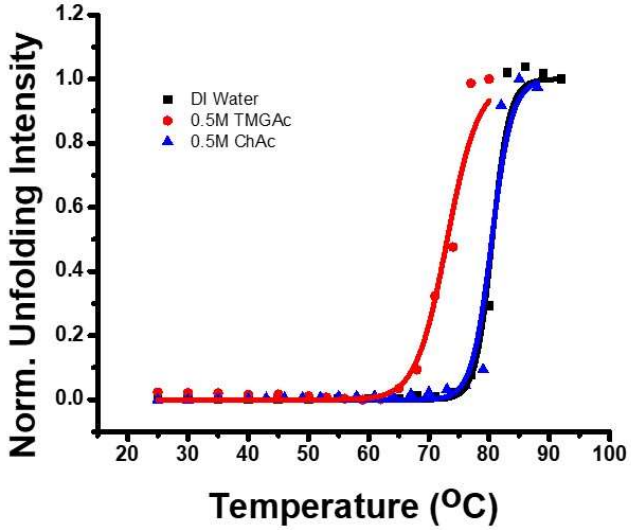

Figure 2.13. Control unfolding experiments with azurin in ILs with small Ac^- anions.

In reference to AAILs used, there are some essential AAs that were not used. They either did not dissolve well at the proper concentration, or they were not easily available. The AAs used all encompassed a select few of the specific side chain properties, enough to interpret which properties affected the protein the most or the least. It appears the nonpolar and the positively charged side chains have the most effect on the azurin protein. It also seems that with choline as the cation, the positively charged AA side chain had the strongest destabilization effect. And a median destabilizing effect came from the hydrophobic effect of the valine (Val) AA side chain. It appears the opposite effect is true for the TMG cation where Val had the strongest destabilization effect and lysine (Lys) had a median destabilization effect. It is possible that the structure of TMG has a very specific interaction to induce Val to be the strongest destabilizing AA side chain. TMG as its cation form has 2 protons connected to the positively charged nitrogen in the structure and may affect the azurin structure by interfering with the H-bonds in the azurin-water interaction, allowing hydrophobic AA side chains to have a stronger effect. While choline is a tertiary amine in its cation form, which may not form as many H-bonds to interfere with the azurin-water H-bonds and alluding to a weaker interaction on the azurin protein as ChVal. However, Lys, a positive side chain AA, had a stronger effect when present as a ChAAIL specifically, which may indicate that the positive Lys with choline, caused an increase in the destabilization effect.

The data from Figure 2.12 contains unfolding curve control experiments directly comparing TMG and choline cation. In Figure 2.12, there is no curve fit to the ChCl unfolding data because the azurin did not completely unfold, so there was some slight stabilization from ChCl. There was very little destabilization from the AAILs in Figure

2.12, but there was a small amount of destabilization more from TMGCl than ChCl. It is less prevalent but still present in Figure 2.13 with TMGAc and ChAc. Showing more destabilization from TMGAc than ChAc. It is possible that the TMG cation with the extra hydrogen, leading to its cation form, causes enough interaction with the residues on the azurin protein to cause differing effects from the ChAAILs, but this is simply speculation.

These ions could be impacting the tertiary structure of the azurin protein through an impact by ionic strength, but past studies have shown that this is not always the case.[87] Scholtz and coworkers have shown that ionic strength can have either an increase in stability or decrease in stability of α-helical domains depending on concentration which is consistent with the understanding that the effect of ions on tertiary structure is not one size fits all from protein to protein.[87] Even the Hofmeister effects can only fit a subset of ionic effects on proteins and explains the interaction between protein-water from the ion perspective. This is partially the understanding gleamed from this study, but the trends show another likely story. For example, studies on myoglobin show that ILs that have an increase in ionic strength do not have a larger effect on myoglobin unfolding than NaCl.[57] Another study, completed by Dominy et al, shows that bacteria that are acclimated to lower temperatures (mesophiles) and their proteins that were subjected to various salt concentrations for testing ionic strength effects on protein stability, showed that their proteins were stabilized with increasing ionic strength.[88] Azurin is found in *P. aeruginosa* naturally which is also a mesophile, so according to this study, the protein should be stabilized with increasing ionic strength (above 200 mM) but this is not the case in this study.[12 89] So, clearly other effects have a larger impact on the protein thermal stability and cause destabilization. One can think of Hofmeister effects as a template to build an

understanding of the observed trend, and then utilize knowledge on basic intermolecular forces (IMFs) from a structural standpoint to explain the trend herein.

In reference to the destabilization effect, proline clearly has a strong effect whether in the presence of TMG or choline. Valine has a stronger destabilization effect as an anion pair with TMG as opposed to choline. This is possibly because of the previously mentioned effect with TMG as opposed to choline, but that is only speculation and would need to be confirmed through repeated tests with choline and TMG cation on the thermal unfolding of the azurin protein. The opposite effect occurs with Lys as anion pairs with TMG having a much weaker destabilization effect, but with choline, it has a very strong destabilization. This could occur depending on the pH of the solution of ChLys or TMGLys at the time of synthesis. This may affect the number of Lys molecules that form the AAIL with either TMG or choline and, depending on pH of the final solution, could cause a completely different thermal effect. Choline is in its basic form when first added to the amino acid when dissolved in water, which may mean that many Lys molecules shift to their anionic form and easily form ChLys. But, with TMG, the Lys added was in its protonated state (LysHCl) which means it would reduce the pH of the solution it is in. As seen in Figure 2.11, there was a set of control data measured utilizing different pH 20 mM ammonium acetate buffers to test pH changes and how they affected the thermal unfolding of the azurin protein. When the solution that azurin dissolves in is both too basic (≤10 pH) or too acidic (≥4 pH) the azurin is slightly thermally destabilized. This means that depending on acidity or basicity of the synthesized AAIL, there could be an impact on the thermal destabilization of azurin. The final pH of the 1 M stock AAIL solutions were not tested, and for future study, observing the pH of the 1 M stock AAIL

would help to infer the pH effect on the protein unfolding. It is possible that in the case of TMGLysHCl the effect was more intensely based on pH and therefore not as strong an effect as ChLys. This helps explain the extreme difference in the destabilization trend of the lysine AA side chain from TMGLysHCl to ChLys, which could lead to further understanding of other AAIL effects.

In comparing Figure 2.5 and Figure 2.6, there is a clear similarity to TMGGly and ChAla. ChAla has a T_m value of 55°C and TMGGly has a slightly lower T_m of ~50°C. Glycine (Gly) contains only an extra proton as its side chain, while alanine (Ala) has an extra methyl group for its side chain. Because they are similar and separated only by 1 carbon and 2 extra hydrogen atoms, this may be what is causing the increased stabilization, but the increased thermal destabilization may also arise from the TMG cation decreasing thermal stability, but further investigation needs to occur to confirm.

Observing the trend of the serine (Ser) and threonine (Thr) AA side chains makes sense as the only difference between the Ser and Thr side chains is a single extra methyl group in Thr. Both TMGSer and TMGThr had a strong thermal destabilization effect on the azurin protein, reducing the T_m to ~52°C. While both ChSer and ChThr had a slightly stronger thermal destabilization than TMGSer and TMGThr, the T_m was reduced to ~47°C. This reveals a similar pattern of reducing the thermal destabilization by ~5°C in relating TMGAAILs to ChAAILs. A similar pattern can be seen when comparing TMGAsp/TMGGlu to ChAsp/ChGlu. Though ChAsp more strongly destabilizes the protein as compared to ChGlu, but AA side chains are so similar that they are only different in structure by one extra methyl group present in glutamic acid. TMGAsp/TMGGlu had a very similar effect that their T_m was at ~65 °C, but the

ChAsp/ChGlu were slightly less destabilizing azurin. The T_m of ChAsp was ~65 ºC and ChGlu was ~70 ºC. This does not exactly follow the trend seen comparing ChAAIL to TMGAAIL, but there is a clear difference in ChGlu which follows the trend. In relation to ChVal vs TMGVal, both cause a strong destabilization in the azurin molecule, but they have a margin of ~20 ºC difference in T_m. Of course, ChVal destabilizes the azurin much less than TMGVal, which is consistent with the conclusion that choline is likely to cause less destabilization. H-bonds likely have a strong impact on stability. It is possible that the presence of more H-bonds in the cation and anion would lead to a decrease in the available water H-bonds that can be made with the protein therefore reducing stability of the protein. Choline clearly destabilizes the azurin protein much less than the TMG cation. This is consistent with the fact that choline is a biologically compatible molecule and should, in theory, cause less thermal destabilization effects on biological proteins.

In comparing AAILs by AA side chain, there is a trend that shows that the AA side chain with a pyrrolidine has a very strong effect on the azurin mixed structure protein. And some of the hydrophobic side chains are causing a median amount of thermal destabilization with the protein structure. While polar side chains cause slightly more destabilization when choline is the cation, but less so when TMG is the cation paired with polar AA. The carboxylic acid AAs tested showed little destabilization with both TMG and choline.

Section 3.1 Enthalpy and Entropy of Unfolding

Of the AAILs tested, the AAILs that fully unfolded the protein were able to be analyzed using the equation found in Figure 2.4. This provided a way to quantify thermodynamic values from the thermal unfolding studies completed on the azurin protein. When using this technique to analyze and fit the unfolding curve to the data points collected, there is a wide margin for error because of the time stipulations for collecting a thermal unfolding experiment. Using the current technique of collecting every ~5 ºC or ~3 ºC provides enough data to fit a line to the curve, but it can only be so accurate. Producing just one thermal unfolding experiment for one AAIL would take hours, and that isn't counting AAIL synthesis and solution prep. For this reason, the thermodynamic values provided are likely not completely accurate. The purpose of these values is to show us a trend of how the ΔS_{unf} and ΔH_{unf} provide a platform for which the study to be strengthened when understanding how these AAILs will affect this mixed structure protein.

Table 2.1

A Table Showing Thermodynamics Data of 0.5 M TMGAAILs.

TMGAAIL	ΔH (kJ/mol)	ΔS (J/mol*K)
DI water	747	2114
TMGPro	480	1539
TMGVal	432	1366
TMGGly	403	1239
TMGThr	417	1276
TMGSer	392	1189
TMGLysHCl	398	1194
TMGGlu	362	1065
TMGAsp	362	1065
TMGAc	383	1106
TMGHCl	484	1381

Note. This thermodynamics data table is organized by decreasing destabilization of 0.5 M TMGAAILs from Figure 2.5 but starting with DI water as our control.

Table 2.2

This Data Table Shows Thermodynamic Values of 0.5 M ChAAIL Unfolding Experiments From Figure 2.6.

IL	ΔH (kJ/mol)	ΔS (J/K*mol)
DI Water	747	2114
ChLys	337	1058
ChPro	689	2121
ChThr	580	1807
ChSer	493	1527
ChPhe	474	1455
ChAla	476	1443
ChVal	434	1305
ChAsp	500	1465
ChGlu	472	1359
ChAc	625	1769

Note. This data set is organized by decreasing destabilization but starting with control of DI water.

As interpreted previously through T_m values, there will be a similar technique for analyzing the ΔS_{unf} and ΔH_{unf} data provided in data tables 2.1 and 2.2 respectively. Data table 2.1 includes all ΔS_{unf} and ΔH_{unf} for 0.5 M TMGAAILs utilized from the thermal unfolding experiments that were provided in unfolding curve format in Figure 2.5. In table 2.2, one can see the ΔS_{unf} and ΔH_{unf} data for 0.5 M ChAAILs that came from thermal unfolding data provided in Figure 2.6. These ΔS_{unf} and ΔH_{unf} values are not easily interpretable because of the wide margin of error, but a trend can be observed. Data tables 2.1 and 2.2 are both organized in the same fashion, starting with the control of DI water, and then going down by decreasing thermal destabilization. So, the AAIL at the bottom of the table destabilized azurin the least and the AAIL second from the top of the table destabilized azurin the most.

The ΔS_{unf} values in data table 2.1 show a decrease in the ΔS_{unf} as there is less thermal destabilization from the TMGAAILs. There is not a large or obvious change in the ΔH_{unf} in the TMGAAIL values for each AAIL. The decrease in ΔS_{unf} as thermal destabilization decreased could be indicative of the H-bonds from the TMG cation interacting with the azurin-water interactions, which allowed for the AA anion to have a strong interaction with a decrease in ΔS_{unf}. H-bond interaction carries a large impact on the energy through ΔS_{unf} because they can impact the organization of energies between AA residues and the water organizational state, leading to a change in unfolding energies. The AA side chain changes the structural effect of the AAIL on the azurin protein. This is consistent with the fact that these AAILs are tunable molecules, impacting the structural order of the protein depending on the AA side chain property that is present in the AAIL.

From data Table 2.2, the ΔS_{unf} value of ChPro very clearly jumps out as an outlier not fitting the trend with data Table 2.1. There is a very clear decrease in ΔS_{unf} with decreasing thermal destabilization on the azurin structure consistent with ChAAILs, aside from ChPro. But something worthy of note is that ChAAILs ΔS_{unf} values do not decrease as remarkably as TMGAAIL ΔS_{unf} values did. This could be because choline is a more biologically compatible cation as compared to TMG. Or this could be because choline is a tertiary amine and does not have as strong of an interaction to the AA residues on the azurin protein like TMG will with its ability to form 2 H-bonds per TMG cation. Overall, the majority of the TMGAAILs and ChAAILs have a strong thermal destabilization effect on the mixed structure of azurin.

Chapter 3

Fundamental Thermal Destabilization Studies on the Protein mCherry With Both Choline and TMG Amino Acid Ionic Liquids (AAILs)

Section 1 Introduction

This chapter is a discussion regarding all AAILs tested on the protein mCherry. As mentioned previously, the mCherry protein is a biologically engineered protein, originating from the protein dsRed found in specific coral species.[90] The purpose of using another protein to study the effects of these AAILs is to obtain further understanding on AAIL physicochemical effects on a different protein structure. Not all proteins share the same structure or properties. The azurin protein was a mixed structure protein which means it has multiple common protein structures. The mCherry protein specifically contains only the β-barrel structure, as can be seen in Figure 1.3, which is a unique protein structure.[11] To gain further understanding on how AAILs influence the thermal stability of the β-barrel structure will lead to a broader understanding of these tunable AAILs on proteins for therapeutics or other protein-AAIL applications in industry.[2 3 8 79] This plans to be analyzed through an organizational analysis by AA side chain property and directly relate to protein-IL and protein-water interactions that lead to destabilization. Some of the industry applications contain those of pharmaceuticals, cosmetics, or therapeutics.[3 5 8 9] RFP (or mCherry) is also a very useful and easy to access protein because the synthesis and purification procedure is very simple and accessible. The mCherry protein is a model protein for identifying how AAILs impact more unique and specific protein structures. Involving data that includes thermodynamics and

understanding thermal stability effects, helps us to identify the trend of AA structure effects in the AAILs tested on this unique β-barrel structure.

Section 2 Experimental Data

As the structure of mCherry, shown in Figure 1.3, the protein itself unfolds at 72ºC in a buffered environment. The experiments completed in this thesis utilized CD spectroscopy to identify the specific tertiary structure, as well as the chromophore (579 nm) of mCherry, and this can be seen in Figure 1.4. The two positive peaks, identified at 265 nm and 345 nm respectively, are the tertiary structure specific to mCherry. The absence of these peaks is how we differentiate unfolded mCherry protein from folded protein in the studied sample. The absence of the negative chromophore trough gave rise to understanding that the chromophore was no longer absorbing light when the peak went to zero. It has been observed that some AAILs can reduce the chromophore, it can easily be reduced by reducing agents as has been seen before.[91] It was recognized that some AAILs would have an effect on only the chromophore of the mCherry solution. This is because the color of the solution would change and when testing the solution in the CD spectrometer, the chromophore peak at 579 nm would be absent while the other two positive peaks were still present. This proved that the mCherry protein was still folded but was being reduced by the AAIL. This was the main reason that the group decided to start utilizing activated charcoal, to both decolorize the AAIL solution and prevent the AAIL from reducing the mCherry chromophore.

To understand its physicochemical effects, each AAIL sample tested on mCherry was put through a thermal unfolding experiment outlined in the introduction section. Typical thermal unfolding experiments would involve 1 mg/mL mCherry solutions with

0.5 M AAIL present and allowed to unfold from 25 ºC – 95 ºC. The data collected after every CD thermal unfolding experiment was analyzed by integrating the area under each positive peak at 265 nm and 345 nm. After integrating the area under each peak for each temperature value, the thermal unfolding curve was generated like Figure 2.3. A control experiment was performed involving mCherry in PBS (20 mM phosphate buffer saline) and various ammonium acetate buffers at pH values ranging from a pH of 4 to a pH of 10. This can be seen in Figure 3.1. Figure 3.2 is another control figure, showing a comparison of mCherry unfolding in the absence of AAILs, with choline or with TMG cation. Figure 3.2 is meant for comparing cation to cation and seeing the change in effect on mCherry protein without AA side chains present. A summary of all 0.5 M TMGAAILs tested with mCherry can be seen in Figure 3.3 where these curves were fit to the integrated and normalized data points for each temperature value. This summary shows an easy comparison of the TMGAAILs that destabilized the mCherry β-barrel structure and those that did not. A similar summary can be seen in Figure 3.4, showing a summary of all 0.5 M ChAAILs tested on mCherry and the AAILs that destabilize the protein strongly or not at all.

Next, these data from Figures 3.3 and 3.4 were analyzed and scaled to 500, to have all unfolding curves start on the same value and show the intensities of the area under the positive 265 and 345 nm peaks. The T_m values for the 0.5 M TMGAAILs tested on mCherry were all collected and organized into two separate scatter plots. Figure 3.5 is a scatter plot of all 0.5 M TMGAAILs T_m values organized by decreasing destabilization but starting with the control buffer. A similar pattern is used for Figure 3.6, showing all 0.5 M ChAAILs T_m values tested on mCherry and organized by decreasing

destabilization. This data set shows the phosphate buffer control T_m first. The next set of T_m scatter plots are the same data from Figures 3.5 and 3.6 but organized in a different fashion. The AAs used in TMGAAILs are not the exact same as the AAs used for ChAAILs, but the AAs with similar side chain properties were put in the same order. For example, Figure 3.7A is organized like the way the AAs are organized from Figure 2.9, from the top left of Figure 2.9 to the bottom right of the figure. In Figure 3.5, the T_m values are 0.5 M TMGAAILs tested on mCherry organized by decreasing destabilization. In Figure 3.7B the T_m scatter plot is organized the same way as Figure 3.7A, but instead utilizing the values from the 0.5 M ChAAILs tested on mCherry. The figures mentioned thus far in this chapter are necessary to outline how the study was performed and organized to observe the trends in the AAILs.

The final data sets in data Tables 3.1 and 3.2 are data derived from the fitting functions from each normalized unfolding curve. These values are thermodynamic values that are meant to provide a trend and not obtained for accuracy, but to identify AAILs that have a strong or weak effect on the β-barrel mCherry protein structure. AA side chain properties and common patterns can be easily observed from unfolding thermodynamic values of each AAIL tested.

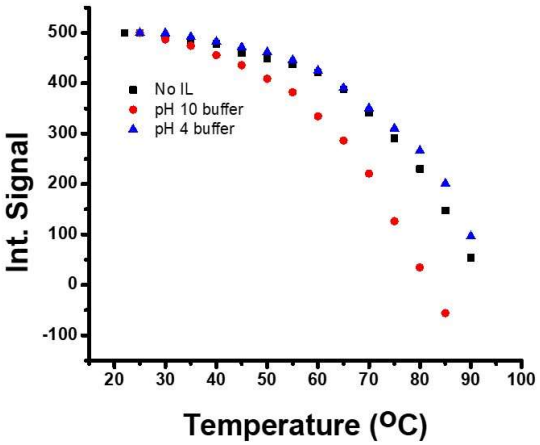

Figure 3.1. A control thermal unfolding experiment including tests run with both pH 10 and pH 4 environments for the mCherry protein to be tested.

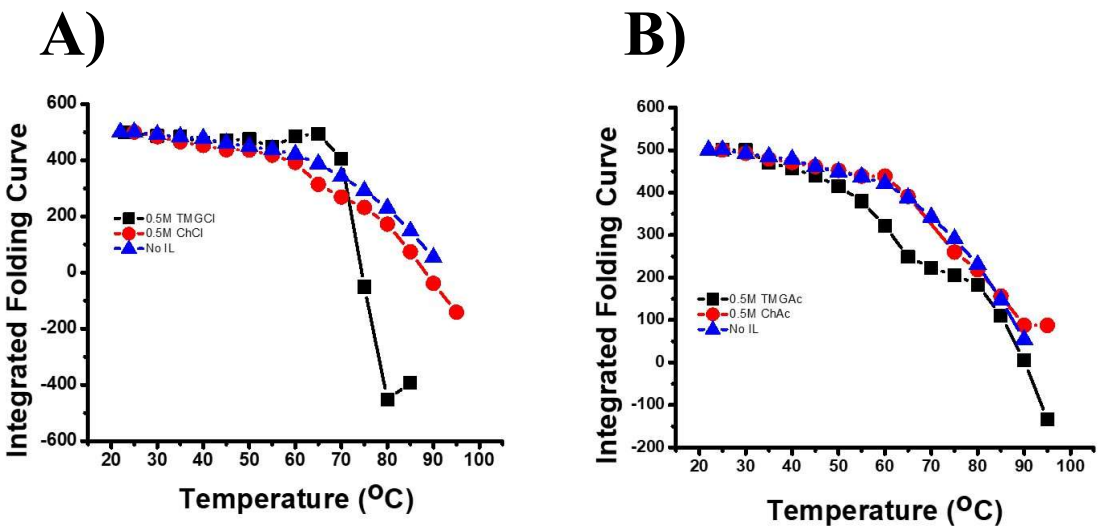

Figure 3.2. This is a set of control experiments, to observe the impact of (A) the unfolding experiments for TMG and choline cation in the presence of a Cl^- and (B) the effect of these cations with Ac^- which is the main ion present in the pH 10 control experiment.

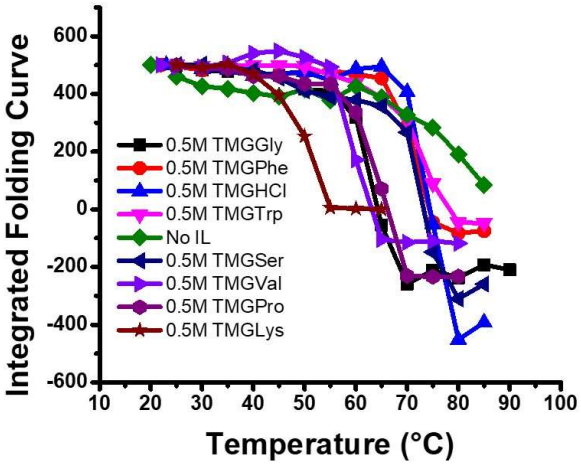

Figure 3.3. This is a summary data set showing all unfolding curves of 0.5 M TMGAAILs of 1 mg/mL RFP, scaled to an intensity of 500, the inflection points still show the T_m values like normalized unfolding curve summaries.

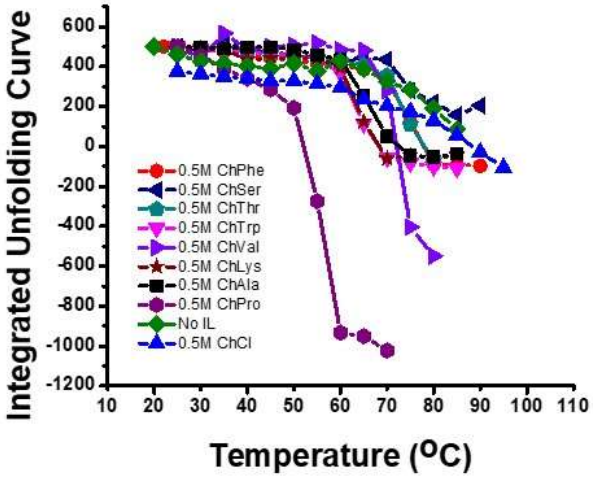

Figure 3.4. This is a summary data set of 0.5 M ChAAILs of 1 mg/mL RFP thermal unfolding curves. These data have been scaled to an intensity of 500.

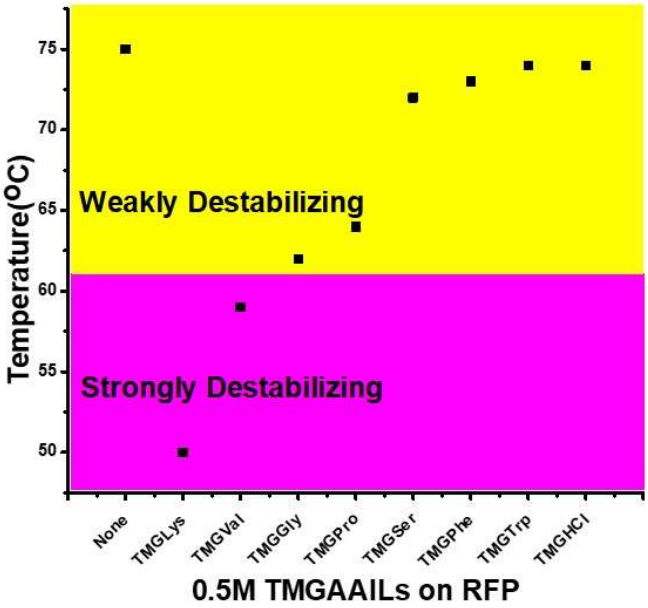

Figure 3.5. A figure showing melting temperatures (T_m) of 0.5 M TMGAAILs in the presence of 1 mg/mL of RFP from Figure 3.2 organized by decreasing destabilization.

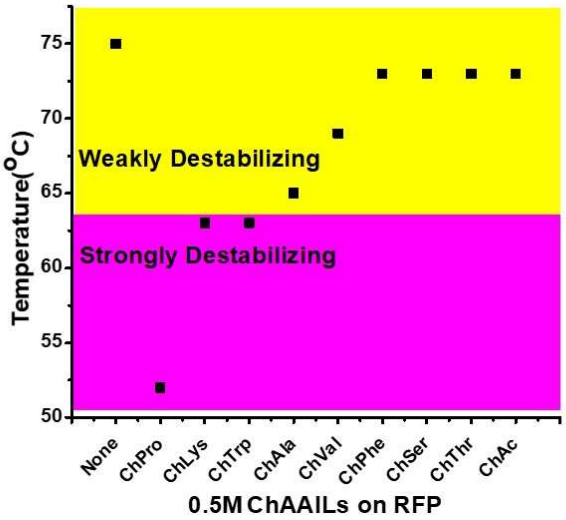

Figure 3.6. A figure showing T_m values of 0.5 M ChAAILs in the presence of 1 mg/mL of RFP from Figure 3.3 organized by decreasing destabilization.

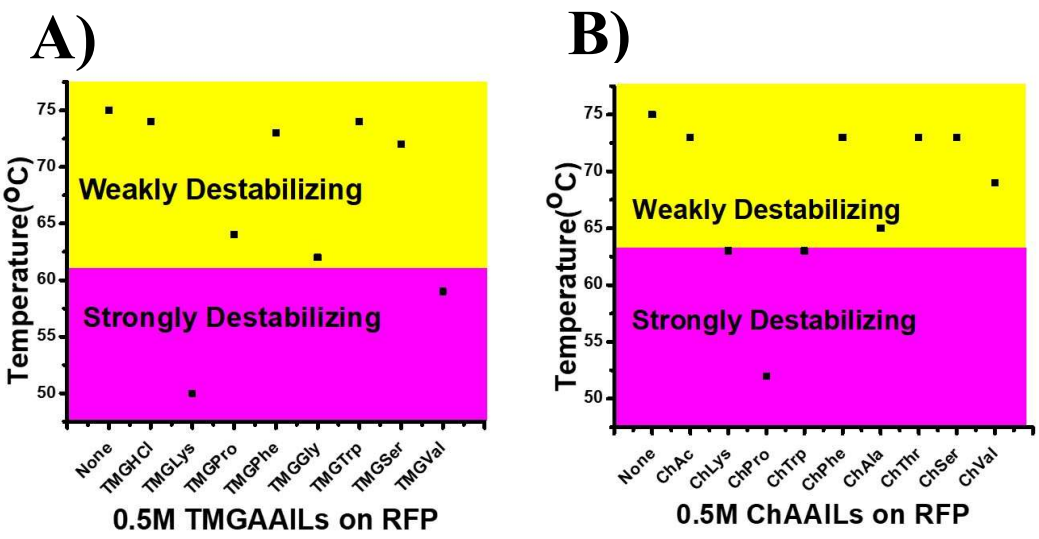

Figure 3.7. A figure showing T_m values of (A) 0.5 M TMGAAILs organized by AA side chain property to match with (B) T_m values of 0.5 M ChAAILs organized by AA side chain.

Section 3 Discussion

The next step to take involves discussing the trends and observed effects of the AAILs on the mCherry protein based on the results of the study. After reviewing Figures 3.3 and 3.4, we can easily compare TMGHCl directly to ChCl. These ILs are essentially control experiments to observe the effect of only the cation as the anions in these cases provide little effect on the protein compared to TMG or choline. A similar experiment was run with TMGAc and ChAc to further understand the effect of TMG and choline cation. Comparing both data sets, the Cl^- in this case would act similarly to NaCl in salt solution, and Ac^- would be acting in a similar fashion to Ac^- in the 20 mM ammonium acetate pH 10 experiment which showed a small amount of destabilization. In this comparison, the TMGHCl clearly caused a small destabilization compared to ChCl and "No IL" which did negligible destabilization. This could be due to the structure of TMG in its cation form, which has two protons with possibilities of forming H-bonds with any AA residue on the β-barrel protein structure or, pulling away water molecules from the protein surface causing slight destabilization. While the structure of choline is a tertiary amine which is not particularly a structure that will have a strong effect on amide bonds, most amino acid residues or on protein-water interactions. For these reasons, TMG could have a stronger destabilization compared to choline, which may change the strength of the effects that AAs may have on the mCherry β-barrel structure. Any slight difference in cation structure can have an impact on the anion's physicochemical effect on the mCherry structure and vice versa. This is in congruence with knowledge on Hofmeister kosmotrope and chaotrope cation/anion. This is a known possibility and the knowledge of choline and TMG being kosmotrope or chaotrope is not yet fully understood.[53] [54] An

overall observation of both Figures 3.3 and 3.4 provides a glimpse into the understanding that the ChAAILs tested do not have as strong as a destabilizing effect as TMGAAILs of the same concentration. This agrees with the idea that because choline is more biodegradable and biocompatible that ChAAILs will least likely thermally destabilize protein tertiary structures compared to the TMG structure. [15 22 51]

Although choline has a weaker destabilization effect on mCherry than TMG, the AA side chain effects do not match with TMG vs choline. For example, when reviewing Figures 3.3 and 3.4, there are 3 ChAAILs that had a strong destabilization effect on mCherry in comparison to TMGAAILs which were only two that strongly destabilize the mCherry β-barrel structure. By T_m value alone, it can be said that proline clearly affects the mCherry protein structure, either as a TMGAAIL or a ChAAIL, but more strongly in the presence of choline. Simply comparing TMGLys to ChLys, both had a strong thermal destabilization of the mCherry protein, but it seems as their effect flipped in the presence of TMG to choline, this may be due to the fact of TMG containing H-bonds and choline not containing as many H-bonds, influencing the effect of the H-bonds contained in the Lys side chain depending on the cation present. Overall, TMGLys has a stronger effect than ChLys, and TMG has more H-bonds which may indicate mCherry thermal stability being affected by the H-bonds in both the structure of TMG and the Lys AA side chain.[84 85] This explanation may be consistent with the Pro AA side chain effect from TMG vs choline. The H-bonds in proline are interacting with the carbonyl side chain that is negative which means that it may not have as much of an interaction with other H-bonds, which can explain the reduced effect in TMGPro. But the opposite occurs with ChPro having a very strong destabilizing effect on RFP. Proline is a unique AA side chain in

which the H-bonds on the nitrogen in the pyrrolidine can form H-bonds with any H—N, H—F, and H—O structure that is present. In TMG, there are lots of N—H bonds present and may reduce the H-bonds ability to interact with the protein-water interaction that stabilizes most proteins.[92] When Pro is in ChAAIL form, the H-bonds are more freely allowed to interact with the environment, in which RFP is present and ChPro strongly destabilizes the RFP. This is reinforced with research done by Krishna et al, stating, "The majority of H-bond forming proline residues occurred in the loop region."[92] This could mean that the ChPro AAILs interact with the loop region of the mCherry protein, pulling H-bonds from the protein-water interaction, causing a strong destabilization effect. Another AA similar in structure to proline is tryptophan (Trp) which had a strong effect as ChTrp but a very weak effect as TMGTrp. This could be for a similar reason as ChPro vs TMG Pro, where the H-bonds available in Trp are one less than in Pro. This leads to Trp having an overall weaker thermal destabilization as compared to Pro which has one more H-bond. This change in destabilization effect can be seen in Figure 3.7A and B. This means that TMGPro and ChPro are more strongly thermally destabilizing the mCherry protein over TMGTrp and ChTrp. But again, TMGTrp would induce a weaker destabilization because the TMG H-bonds are interacting with the AAIL AA reducing their ability to interact with the mCherry protein-water interaction and cause destabilization. Furthermore, ChTrp has a stronger effect because the tertiary amine is not interacting with the H-bonds on the side chain of Trp and therefore allowing them to interact with the mCherry protein-water H-bonds and have a stronger destabilization effect. This pattern can be easily observed from Figure 3.7A and B. This may have a strong indication that H-bonds play a strong role in thermal destabilization of proteins.

This makes logical sense as properties of side chains, like amount of H-bonds, influence the stability of a tertiary structure in a protein and how it interacts with water around it, maintaining its 3-dimensional structure.

To further describe trends that have been observed in Figures 3.7A and B, one can see in Figure 2.9 that alanine (Ala) and glycine (Gly) have very similar structures and therefore similar hydrophobic effects. As mentioned previously, hydrophobic effects are important for protein folding but not as impactful for protein unfolding.[83 84] This is consistent with the results found in this thesis, as TMGGly and ChAla did not have a very strong destabilizing effect on the mCherry tertiary structure leading to unfolding. ChAla and TMGGly are similar enough in AA side chain structure to show the general hydrophobic effect was present to cause some destabilization, but not enough to cause as strong destabilization that H-bonds had caused. ChAla has a T_m value ~65 ^oC and TMGGly has a T_m ~63 ^oC which can be seen in Figure 3.7A and B. Side chains with a weak hydrophobic effect caused a weak destabilization effect.

Another similar AA side chain is phenylalanine (Phe) which contains a phenyl functional group which leads to π-bond interactions along with some weak hydrophobic interactions. As observed through Figure 3.7A and B, there is little to no thermal destabilization from the aromatic AA side chain in TMGPhe and ChPhe form. This is consistent with findings thus far that H-bonds have the strongest impact and hydrophobic effects do not have a very strong impact on mCherry thermal stability.

While Ala only has one methyl group, valine (Val), another AA side chain like Ala, has another 2 methyl groups attached to the side chain of the AA as compared to Ala. This means an increase in hydrophobicity. After observing the T_m values of both ChVal

and ChAla from Figure 3.7A and B, an increase in hydrophobicity indicated a decrease in thermal destabilization. This means that ChAAILs with hydrophobicity have a thermal destabilization effect larger than hydrophilic ChAAILs but increasing hydrophobicity does not necessarily mean more thermal destabilization from ChAAILs. TMGVal had a much stronger effect on the mCherry β-barrel structure. In alignment with how H-bonds in TMG allow interactions of the AA anion to occur with differing effects, the TMGVal caused a much stronger thermal destabilization of ~15 ^{o}C on the mCherry tertiary structure. This means that as TMG interacts with mCherry's protein-water interaction with its H-bonds, the hydrophobic side chain of Val was able to cause a destabilizing effect, but choline did not cause as strong an effect because the mCherry β-barrel and water interaction was not being disrupted by the H-bonds from TMG.

Serine (Ser) and threonine (Thr) both have a similar side chain structure, with only the difference of one extra methyl group on the Thr side chain. There are very similar effects of ChSer vs ChThr and this is indicated by the T_m values of ChSer and ChThr not differing significantly. This is consistent with the understanding that AA side chains with very similar properties/structures will lead to a similar thermal destabilization effect.[46 93] As compared to results from chapter 2 on azurin, there is a difference in the strength of AAIL effect, which is clearly coming from the strength of the effect of AA side chains on azurin's mixed structure vs mCherry's strong β-barrel structure.

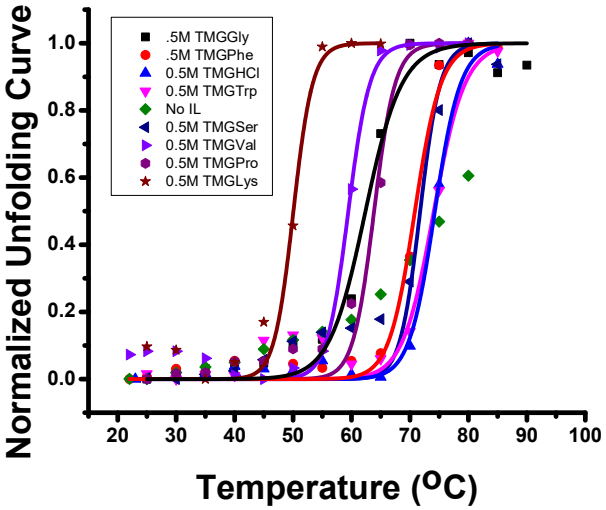

Figure 3.8. This figure shows a normalized unfolding summary of 0.5 M TMGAAILs in the presence of 1 mg/mL RFP.

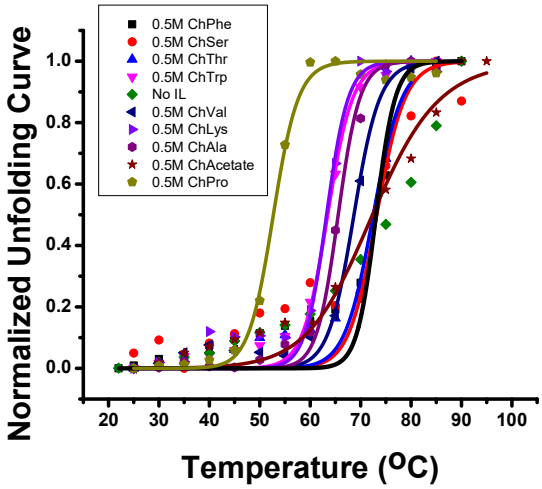

Figure 3.9. This is a normalized unfolding summary of 0.5 M ChAAILs in the presence of 1 mg/mL RFP.

Section 3.1 Enthalpy and Entropy of Unfolding

The data collected in Tables 3.1 and 3.2 are ΔS_{unf} and ΔH_{unf} values that come from the equation found in Figure 2.4. These data sets are only to provide a glimpse into what may be affecting the interaction between the AAIL and the protein the most, enthalpy or entropy and any trends that can be observed. The data in Tables 3.1 and 3.2 are organized by decreasing thermal destabilization. This means that the last set of ΔS_{unf} and ΔH_{unf} in table 3.1 and 3.2 are the AAILs that destabilized the mCherry protein the least. The first set with no AAIL is not present in these data tables because the mCherry protein unfolded but there was not enough data past its unfolding point to fit a line to the unfolding curve found in Figures 3.8 and 3.9. Data Table 3.1 includes all 0.5 M TMGAAIL ΔS_{unf} and ΔH_{unf} values from the unfolding assays in Figure 3.8. While data Table 3.2 are all 0.5 M ChAAIL ΔS_{unf} and ΔH_{unf} values from the unfolding assays in Figure 3.9.

In data Tables 3.1 and 3.2, we can try to follow the trend in ΔS_{unf} and ΔH_{unf} values like the analysis technique used in chapter 2. The TMGAAILs ΔS_{unf} and ΔH_{unf} values were slightly larger than the ΔS_{unf} and ΔH_{unf} values of ChAAILs found in data table 3.2. When comparing ΔS_{unf} and ΔH_{unf} values of TMGAAILs vs ChAAILs, one can see that TMGGly does not follow the trend, but all other TMGAAILs have a decreasing trend of ΔS_{unf} by decreasing destabilization. ChAAILs do not follow the same trend as TMGAAILs, instead there is a clear outlier, that ChPhe caused the largest ΔS_{unf} and ΔH_{unf} values, but aside from this, most ChAAILs cause very similar ΔS_{unf} and ΔH_{unf} values. This may be from the consistency of choline not having a strong effect on the mCherry β-barrel structure due to choline tertiary amine structure. The overall understanding for why

ΔS_{unf} decreases with decreasing destabilization may elucidate the interaction between the protein, the solvent, and the AAIL.

If ΔS_{unf} values decrease with decreasing thermal destabilization by AAILs, this would mean that the entropy to unfold the protein gets smaller as destabilization decreases. This indicates that the largest entropy in a data set comes from the AAIL that causes the most destabilization because the protein is unfolding at a lower temperature and requires less enthalpy, so entropy must be larger to allow ΔG_{unf} values to become negative and be spontaneous. Not only this, but the amount of disorder must be larger at a lower T_m value, to allow this thermal destabilization of the mCherry protein. The generally accepted understanding of thermal unfolding occurring with proteins as temperature increases comes from less water molecules tied down in regions of ordered water molecules around nonpolar side chains.[93] This may elucidate the idea that side chains in AAILs with more H-bonds pull away more water molecules and could cause a further thermal destabilization in the presence of TMG. because choline is a tertiary amine, and the nitrogen on choline does not have as many H-bonds to interact with the H-bonds on the AA side chains therefore the overall the ΔS_{unf} values are smaller for ChAAILs. Unlike with TMG, that has more H-bonds to interact with the AA side chains in the TMGAAIL form, and therefore elucidates more disorder and further destabilization overall.

Table 3.1

Thermodynamic Values (ΔS_{unf} and ΔH_{unf}) of 0.5 M TMGAAILs Unfolding Experiments With mCherry Protein.

AAIL	ΔH (kJ/mol)	ΔS (J/mol*K)
None	--	--
TMGLys	527	1632
TMGVal	499	1500
TMGGly	302	900
TMGPro	524	1555
TMGSer	572	1660
TMGPhe	443	1289
TMGTrp	378	1089
TMGHCl	456	1313

Note. These values were derived from the thermal unfolding summary above in Figure 3.8 and organized by decreasing destabilization.

Table 3.2

Thermodynamic Values (ΔS_{unf} and ΔH_{unf}) of 0.5 M ChAAIL Unfolding Experiments With mCherry Protein.

AAIL	ΔH (kJ/mol)	ΔS (J/mol*K)
None	--	--
ChPro	357	1097
ChLys	439	1306
ChTrp	380	1130
ChAla	446	1317
ChVal	379	1110
ChPhe	526	1520
ChSer	356	1026
ChThr	350	1014
ChAc	150	434

Note. These values were derived from the thermal unfolding summary in Figure 3.9 and organized by decreasing destabilization.

Chapter 4

G-quadruplex DNA With Imidazolium Chloride (ImCl) ILs

Section 1 Experimental Data

As can be seen in the introduction of this work, one can observe the many structures utilized in the work for this chapter. In Figure 1.8 you can see the chemical structures of the imidazolium ILs used organized by length of alkyl chain. In Figure 1.5, one can see various representations of G-quadruplex DNA. In the top of Figure 1.5, one can see a cartoon representation of the G-quadruplex DNA molecule with the tetrads in purple. In the bottom of Figure 1.5 one can see the structure of the G-quadruplex DNA with K^+ represented as yellow balls, and the bottom right one can observe the G-quadruplex DNA without the K^+ ions to stabilize the structure.

Many of these results are coming from a soon to be published paper from the Vaden research group. CD spectroscopy is a very useful technique for observing any changes in the 3-dimensional structure of the G-quadruplex DNA molecule. This also makes it very useful for identifying stability of the molecular structure. This can be seen in Figure 4.1A where the CD spectra of G-quadruplex DNA at 5 μM with and without K^+ is shown. Both spectra exhibit a positive peak at ~260 nm and a negative peak at ~240 nm. As has been reported previously, this spectral signature indicates parallel G-quadruplex structure.[35 38] The CD signal intensity is significantly lower without K^+ which strongly suggests that the population of structured DNA is much lower without the K^+. This is consistent with literature reports detailing how alkali metal ions stabilize the quadruplex structure.[94 95 96]

Figure 4.1B shows the results of a thermal unfolding experiment for G-quadruplex DNA in the presence of 0.5 M [OMIM]Cl (with K^+ as an example). At temperatures above ~55 ℃ the CD signal decreases in intensity and disappears by 80 ℃, indicating that the DNA structure is denatured at high temperature. These spectra can be used to quantitatively measure thermal stability by analyzing the integrated CD signal between 220 and 300 nm as a function of temperature as shown in Figure 4.1C. In this figure, it is noted that the CD signal at 25 ℃ is significantly lower and the G-quadruplex unfolds at a much lower temperature without K^+ present. This figure clearly and quantitatively shows that the G-quadruplex DNA structure loses thermal stability without K^+, as is consistent with the literature.[95 96]

Figure 4.2 shows the results of a CD-based thermal unfolding experiment for G-quadruplex DNA without K^+ in the presence of 5 different imidazolium chloride ILs. Figure 4.2A demonstrates that the ILs do not hinder the CD spectroscopic measurements as this data is 5 μM QDNA with 0.5 M [OMIM]Cl. Figure 4.2B clearly shows that some ILs increase the G-quadruplex thermal stability while others have negligible effects. Any shift of the normalized unfolding curves to the right indicates thermal stabilization. Notably, the shorter-chain ILs ([EMIM]Cl, [BMIM]Cl, and [HMIM]Cl) do not stabilize the structure while the longer-chain ILs ([OMIM]Cl and [DMIM]Cl) stabilize the structure. The two longer-chain ILs are also notably the only ILs that form micelles in aqueous solution.[97] It is reasonable to assume that the micelle-forming ability of the ILs is related to their stabilizing effects on the G-quadruplex structure.

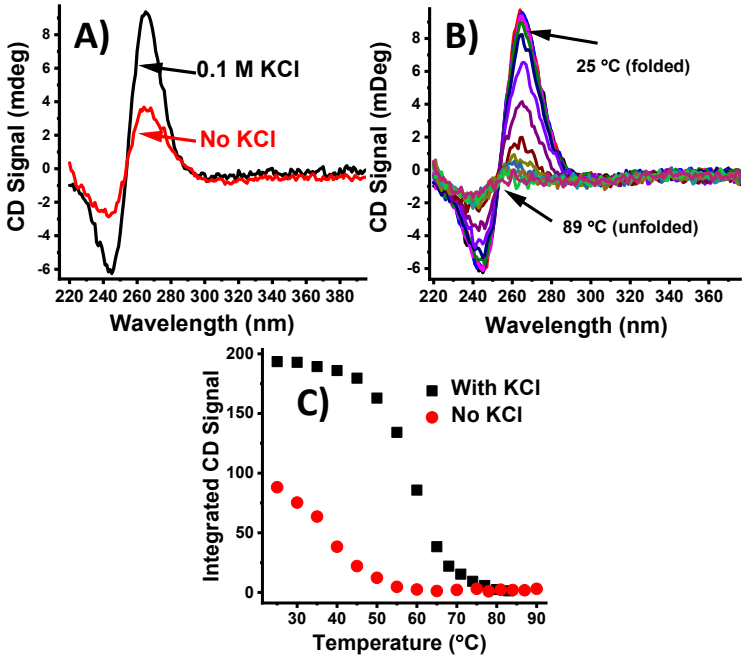

Figure 4.1. This is data showing A) room temperature CD spectra of 5 µM G4 DNA with 0.1 M KCl and without KCl B) a thermal unfolding assay of G4 DNA with K^+ showing all spectra at temperatures from 25 ºC to 89 ºC and C) thermal unfolding curves showing intensities of 5 µM G4 DNA thermal unfolding experiments with and without KCl.

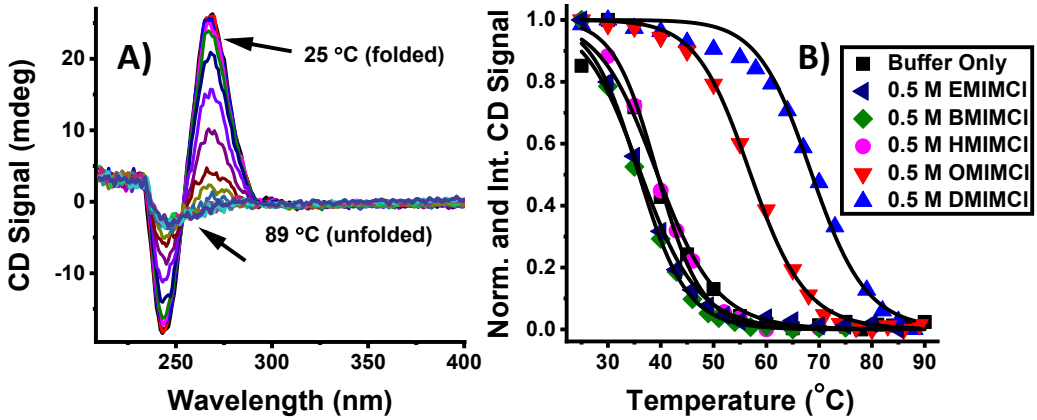

Figure 4.2. (A) thermal unfolding experiment shown above without KCl in the presence of [OMIM]Cl and B) normalized unfolding curves of all ImCl ILs tested on G4 DNA without KCl.

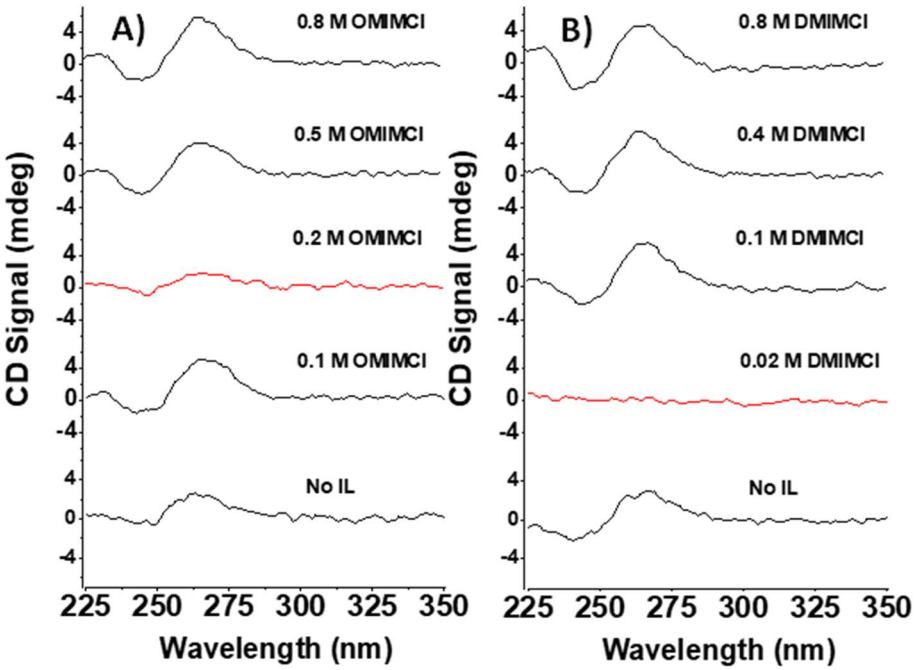

Figure 4.3. CD spectra of 5 mM G-quadruplex DNA with increasing concentrations of ILs. The data measured at IL concentrations equal to the CMC value is shown in red. (A) [OMIM]Cl; (B) [DMIM]Cl.

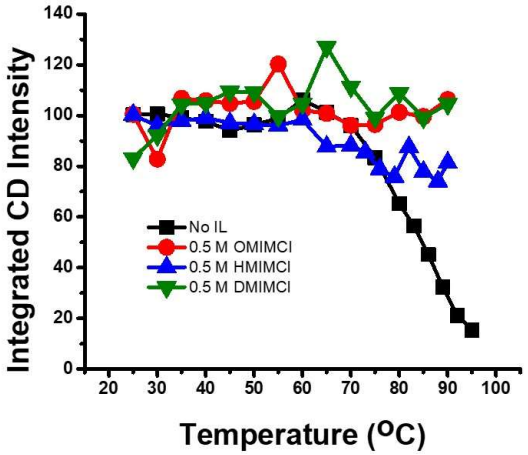

Figure 4.4. Figure showing unfolding curves of 5 μM G-quadruplex RNA in a buffer with 0.1 M KCl, showing data sets of no IL, [HMIM]Cl, [OMIM]Cl, and [DMIM]Cl at 0.5 M. This data was integrated and scaled to 100.

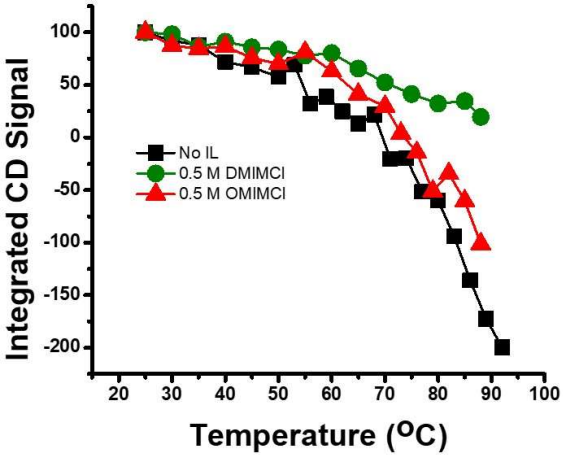

Figure 4.5. Unfolding curves integrated and scaled to 100 without fits for 5 μM G4 RNA without KCl present, for no IL, 0.5 M [OMIM]Cl, and 0.5 M [DMIM]Cl.

Figure 4.3 shows the CD spectra (at 25 °C) for G-quadruplex DNA with increasing concentrations of [OMIM]Cl (Figure 4.3A) and [DMIM]Cl (Figure 4.3B). The critical micellar concentration (CMC) values are 0.2 M and 0.02 M for [OMIM]Cl and [DMIM]Cl, respectively.[98] Figure 4.3 shows that at IL concentrations below their respective CMC values, the G-quadruplex structures are present although at low intensity, and at IL concentrations above their CMC values, they are retained, and present at higher intensity. However, at IL concentrations equal to their CMC values, the G-quadruplex DNA structure is almost completely lost.

One can see in Figure 4.4 analyzed unfolding experiments of 5 μM G-quadruplex RNA without IL, [HMIM]Cl, [OMIM]Cl, and [DMIM]Cl at 0.5 M in the presence of 0.1 M KCl. The control was completely unfolded by ~85 ºC and the experiments run with [HMIM]Cl, [OMIM]Cl, and [DMIM]Cl at 0.5 M showed no destabilization on G4 RNA in the presence of K^+ and therefore the ILs had the opposite effect on G4 DNA with K^+. This is interesting as it is followed by a summary experiment with G4 RNA without K^+ in the presence of ImCl ILs in Figure 4.5. This figure shows another summary of 5 μM G4 RNA without KCl present, in the presence of no IL, 0.5 M [OMIM]Cl, and [DMIM]Cl. This again is the opposite effect that 0.5 M [OMIM]Cl and [DMIM]Cl had on G4 DNA without KCl. This can be interpreted that the presence of the extra oxygen atom in the RNA over DNA may have an impact on the stability mechanism that plays a role on G4 RNA with K^+ leading to stabilization, while the opposite effect is observed with G4 DNA to not be stabilized in the presence of K^+ in the G4 core.

The experimental results clearly illustrate that the micelle-forming ILs increase the thermal stability of G-quadruplex DNA in the absence of K^+. At IL concentrations exactly equal to the CMC values the G-quadruplex is unstable but at higher IL concentrations the stability is recovered and increased. This may be indicative of DNA encapsulation by IL micelles. At the CMC values, the ILs do not completely encapsulate the G-quadruplex structure and destabilize it, but at higher IL concentrations the micelles can fully solvate the DNA which increases thermal stability.

Our research group collaborated with another research group at Rowan University to help further strengthen our claim from the experimental results we obtained on the G-quadruplex DNA with ILs. In this collaboration, simulations of the ILs we studied with G4 DNA with and without K^+ to relate experimental results to simulated molecular interactions. Our collaborators, in Chun Wu Research group, were able to simulate the ILs that had the longest alkyl chains and had the most effect experimentally. As noted from Figure 4.3A and 4.3B, we observed some micellar effects and our collaborators had simulated OMIMCl and DMIMCl forming micelles and the results showed consistency with the experimental results. The G-quadruplex DNA was stabilized in the absence of K^+ with OMIMCl and DMIMCl ILs, showing the ILs that form micelles are stabilizing the G-quadruplex DNA.

Section 2 Discussion

In our previous study,[35] we demonstrated the increased thermostability of Pu22 containing core K^+ in [OMIM]Cl ($T_m \sim 90\ ^0C$) as well as [EMIM]Cl, [BMIM]Cl, and [HMIM]Cl (T_m not calculated), likely due to the increased hydrophobic effect by longer-alkyl chain ILs. However, the detailed effects of removing the cation coordination within

the G4 core have not been well characterized. While it is well-known that electrostatic screening within the G4 core by small cations is a crucial contributor to G4 stability, hydrophobic interactions in nucleic acid moieties (e.g., nonpolar nitrogenous bases, π-π stacking interactions) keep the G4 core "dehydrated" from intrusive water molecules, sequestering them to the phosphate backbone. This is also true for other nucleic acid motifs (e.g., double-stranded DNA/RNA), where the space occupied by the VDW interactions does not permit water to enter the hydrophobic core. Occupying K^+ cations also prevent water invasion into the G4 core.

In the absence of core K^+ and zero salt conditions, water can enter the G4 core and contribute negatively to G4 stability; the partial negative charges carried by the water molecules likely confer additional electrostatic repulsion with O6 guanines, hastening G4 collapse. To the best of our knowledge, the potential of hydrophobic media (e.g., long-alkyl chain ILs) in stabilizing cation-deficient G4s hasn't been sufficiently investigated. In this study, the Pu22 G4 without core K^+ had collapsed in zero salt conditions (i.e., buffer, Pu22-No KCl) and in shorter-alkyl chain ILs ([EMIM]Cl, [BMIM]Cl, [HMIM]Cl), but was relatively stable in longer-alkyl chain ILs ([OMIM]Cl, [DMIM]Cl). [OMIM]Cl and [DMIM]Cl are the only two ILs in this study reported to form micelles; from our direct observations, it is strongly suggested that the hydrophobic effect and micellization increased the thermostability of the Pu22 G4 structure.

The exact mechanism of how micelles affect the G4 DNA structure is not completely understood. It is obvious that G4 stability is increased above and below the CMC values of [OMIM]Cl and [DMIM]Cl, but at their exact CMC values, the G4 structure is completely destabilized. This observed destabilization could possibly be due

to the micelles being just the right size to cause destabilization of the G4 DNA structure. The simulations from our collaborator showed aggregating micelles around the G4 structure when at 0.5 M but did not elucidate any exact mechanism and the experimental results cannot provide this alone. Instead, further research for understanding the exact mechanism of micellar formation interacting with G-quadruplex DNA structure would be important for optimizing ILs for stabilizing G4 DNA in nucleic acid therapies and technologies.

It is currently understood that substances like lipid nanoparticles and nucleosomes can play a role in DNA/RNA therapeutics/technologies.[99] [100] [101] Like micelles, lipophilic vesicles repurposed as drug carriers (i.e., lipid nanoparticles (LNPs), liposomes, etc.) also utilize the hydrophobic effect to enhance drug stability and deliverability[99] [101]. For example, the SARS-CoV-2 mRNA vaccines patented by BioNTech (Comirnaty) and Morderna (SpikeVax) are LNP formulations to mediate mRNA delivery to the host cells.[102] In an aqueous environment, the LNP architecture comprises ionizable and neutral phospholipids which form a spherical bilayer, and PEG-lipids and cholesterol to stabilize the LNP structure and mediate endosomal internalization. The nonpolar phospholipid tails orient to the LNP interior to induce the hydrophobic effect. Simultaneously, the head groups of the ionizable phospholipids (positively charged) engage in charge-charge interactions with the negatively charged nucleic acid backbone.[101] This encapsulates individual nucleic acids while screening their charge, lowering the interior net charge of the LNP, and making the hydrophobic effect more prominent. In comparison, IL micelle architecture is simpler, as the components comprise just a small amphipathic cation ($[OMIM]^+$ or $[DMIM]^+$) and a small halogenic anion (Cl-). Sufficient IL cation

concentrations could neutralize the charge of nucleic acid molecules. Hereon, the neutral IL-Cl salt can promote cation-to-micelle formation via the hydrophobic effect.

The understanding provided from G4 DNA could lead to further development with RNA technologies, but with the results provided in Figure 4.4, one can see that the mechanism that caused G4 DNA to be stabilized in the absence of K^+ is not active in impacting the ImCl ILs stabilization effect on G4 RNA in the same environment. Rather, the G4 RNA experienced a stabilization effect by [OMIM]Cl and [DMIM]Cl in the presence of K^+ which was not the case for G4 DNA in the presence of K^+. This could mean that the micelle effect on DNA and RNA could have very opposing interactions, just from the shift of DNA to RNA. The data in Figure 4.5 proves that in the absence of K^+, there is a lack of stabilization on G4 RNA by the ImCl ILs that had stabilized G4 DNA, [OMIM]Cl and [DMIM]Cl. These ILs that form micelle structures clearly have impact on G4 DNA but not on G4 RNA in the same environments from these results. This could mean further study and understanding of the mechanism of micelles on G4 DNA vs G4 RNA should be thoroughly investigated with experimental and simulated results to identify the underlying cause for these opposing results.

Chapter 5

Conclusion and Future Outlook

Section 1 Conclusions and Closing Remarks

In this work, studies were completed involving various ILs that had many physicochemical impacts on biological molecular structures. In this breath, the spectroscopic techniques used helped us to identify the state of the biological molecule (folded vs unfolded), the presence of a tertiary structure (CD spectroscopy), and the thermodynamic values of each IL on the biological molecules to observe a trend. This knowledge provides further insight on ILs, specifically their ability to impact an increase or decrease of thermal stability of a biological macromolecule. This is useful knowledge as the biological molecules studied are optimal molecular models to apply the understanding of IL physicochemical effects on specific structures. This learning provides a way of further understanding the physicochemical effects that ILs can have on biological molecules and their impact on a wide variety of applications, including therapeutics, pharmaceutics, or cosmetics. Some ILs are more biologically compatible than others and the trends learned in this study show the impact some of those ILs have on thermal stability. The patterns that could be observed were backed up by the understanding of the essential amino acids and their side chain properties, as well as through known ImCl IL hydrophobic effects.

In chapter 2, one can see that the effects of AAILs on azurin were organized by AA side chain property and its effect as a TMGAAIL or a ChAAIL. It was concluded that overall, the strongest thermal destabilization effects came from positive side chains and

hydrophobic side chains, with both TMG and choline. Some thought was given on the effect that TMG or choline cation had on the mixed structure of azurin, but the best conclusion to be drawn is that TMG cation has more H-bonds to interact with protein residues that have H-bond interactions with surrounding water molecules, while choline cation has less. This may play a role in the impact that the AA in the AAIL has on the protein and therefore causes such differing effects from TMGAAILs to ChAAILs of the same AA. This is simply speculation, but studies have been done to further understand the exact mechanism of IL interaction with proteins to disrupt protein-water interactions and cause thermal destabilization.[103] There was another understanding gained from Figure 2.11 which proved that there is a small effect of pH on the azurin protein when thermally unfolding. Both low and high pH cause a small destabilization effect. Depending on the pH of the AAIL, as well as the cation TMG or choline, could all play a role on the impact of the thermal destabilization, which is reflected clearly in TMGLys and ChLys.

In comparing AAILs by amino acid side chain, there is a trend that shows that proline's pyrrolidine structure has a very strong effect on the azurin mixed structure protein. This could come from its interaction with rigid loop structures that often also contain proline side chains. Some of the hydrophobic side chains are causing a median amount of thermal destabilization with the protein structure. While polar AA side chains cause slightly more destabilization when choline is the cation, but less so when TMG is the cation. The carboxylic acid side chain AAs tested showed little destabilization with both TMG and choline.

A further understanding can be gained from data tables 2.1 and 2.2. The overarching conclusion is that ΔS_{unf} values decreased with decreasing thermal destabilization effect of AAIL. This applies to both TMGAAILs and ChAAILs but is more obvious with TMGAAILs. There is an outlier, ChPro, but this can come from a bad fitting curve, or from the fact that ΔS_{unf} and ΔH_{unf} in this study are only for observing a trend and not for providing accurate thermodynamic values. Overall, the ΔS_{unf} and ΔH_{unf} values did help provide further strengthening to understanding how AAILs led to observing a pattern in the impact of TMGAAILs and ChAAILs with respect to AA side chain property.

In chapter 3, ChAAILs show that positive AA side chains and hydrophobic side chains have a moderate or strong thermal destabilization effect on the mCherry structure. Regarding TMGAAILs, specifically positively charged side chains, and H-bond forming side chains had a stronger effect with TMGAAILs over ChAAILs. The conclusive results from the ΔS_{unf} and ΔH_{unf} values tell us that the TMGAAILs cause overall higher ΔS_{unf} and ΔH_{unf} values as compared to ChAAILs. This could be from the impact of the H-bonds in TMG in the protein-water interaction causing a larger change in energies as opposed to choline. But overall, both tables 3.1 and 3.1 show that with decreasing thermal destabilization, there is a decrease in ΔS_{unf} values, like chapter 2.

Regarding chapter 4, G-quadruplex DNA has a very specific interaction with ImCl ILs that was unexpected and should be further investigated. The ImCl ILs with the longest alkyl chains [OMIM]Cl and [DMIM]Cl have the strongest stabilization effect on G4 DNA without a metal ion to form the core of the G4 DNA (i.e. no K^+ or Na^+). It was discovered through a concentration dependent assay and through collaboration with a

MD simulations group, that [OMIM]Cl and [DMIM]Cl caused the stabilization of the G4 DNA likely through micelle encapsulation. It is known that these ILs form micelles in aqueous solution. The exact mechanism is not yet known, but it was determined that at the CMC values of [OMIM]Cl and [DMIM]Cl the G4 DNA structure is not present through CD absorbance. This can be seen in Figure 4.3. The current understanding is that above and below the CMC value, the micelles present allow QDNA solvation, but at the CMC value, this does not occur. The G-quadruplex RNA was also researched with [HMIM]Cl, [OMIM]Cl, and [DMIM]Cl in Figure 4.4. It was concluded that [OMIM]Cl and [DMIM]Cl had a stabilization effect on G4 RNA in the presence of K^+ but these ImCl ILs did not have any stabilization effect on G4 RNA in the absence of K^+.

In conclusion, G-quadruplex DNA and G-quadruplex RNA were impacted by micelle forming ImCl ILs. Specifically, G4 DNA was thermally stabilized by micelle forming ImCl ILs in the absence of K^+, but G4 RNA was stabilized in the absence of K^+ This insight will lead to further study of the impact of micelle forming ILs on G-quadruplex nucleic acid structures and how the mechanism of the micelle formation impacts these structures specifically. Regarding chapter 2 and 3, less AAILs had a thermal stability effect on the mCherry β-barrel structure as opposed to the azurin mixed structure. This could be from the strength of the mCherry β-barrel to resist a change in entropy and therefore maintain thermal stability, as opposed to azurin with only a mixture of 1 α-helix and a set of β-sheets. Or this could come from the number of hydrophobic residues on the β-barrel structure, leading to an increase in its ability to resist an impact from the AAILs on the protein-water interaction that keeps the protein thermally stable.

This understanding provides insight on AAILs as useful tunable biomaterials in the various applications of pharmaceutics, cosmetics, therapeutics, and green solvents.

Section 2 Future Outlook

Further study may involve more testing of AAILs on different protein tertiary structures. Involving MD simulations to find the mechanism of action that the AAILs impact to cause thermal destabilization. Different biological monomers to use for ILs, like fatty acids ionic liquids (FAILs) to observe if there are any stabilization effects from micelle forming ILs. Testing AAILs for molecular stability by using MD simulations and then utilizing CD spectroscopy to test stabilization of proteins over time in the presence of AAILs. Further understanding of azurin thermal unfolding being affected by the pH of the IL used when in DI water alone would be another interesting study to gleam the pattern of pH affects. To test ionic strength of AAILs on both proteins, low concentration IL studies would be useful and lead to deeper understanding on more physicochemical effects of these AAILs. Experiments testing AAILs with QDNA and QRNA would be useful to further explore the applications of these novel materials. All of this will help to provide further insight on the knowledge herein expanded upon that needs filling in and can be useful for future therapeutic applications.

AAILs have a massive potential to be useful in applications for stabilizing therapeutics and use as alternative solvents. Their biocompatibility and biodegradability provide a foundation for use in biological therapeutics and possible alternatives to present organic solvents that are highly volatile which lead to environmental hazards like air pollution. The world needs to shift to focus more resources on utilizing new scientific knowledge for future innovations to improve human impact on the environment. Finding

new scientific technology, materials, and techniques are the ways of the future to improve the world around us and leave it better than we found it. Finding the inspiration to focus and get excited for learning and innovation is the path to understanding ourselves and our place in the universe. ILs are just one of the many topics of study that will lead us to an improved perception on medicine, infrastructure, and our environment.

References

(1) Kelleher, N. L. A Cell-Based Approach to the Human Proteome Project. *Journal of the American Society for Mass Spectrometry* 2012, *23* (10), 1617-1624. DOI: 10.1007/s13361-012-0469-9.

(2) Leader, B.; Baca, Q. J.; Golan, D. E. Protein therapeutics: a summary and pharmacological classification. *Nat Rev Drug Discov* 2008, *7* (1), 21-39. DOI: 10.1038/nrd2399 From NLM.

(3) Dimitrov, D. S. Therapeutic Proteins. *Methods in Molecular Biology* 2012, *899*, 1-26. DOI: 10.1007/978-1-61779-921-1_1.

(4) Sattlecker, M.; Kiddle, S. J.; Newhouse, S.; Proitsi, P.; Nelson, S.; Williams, S.; Johnston, C.; Killick, R.; Simmons, A.; Westman, E.; et al. Alzheimer's disease biomarker discovery using SOMAscan multiplexed protein technology. *Alzheimer's & dementia* 2014, *10* (6), 724-734. DOI: 10.1016/j.jalz.2013.09.016.

(5) Lazar, G. A.; Marshall, S. A.; Plecs, J. J.; Mayo, S. L.; Desjarlais, J. R. Designing proteins for therapeutic applications. *Current opinion in structural biology* 2003, *13* (4), 513-518. DOI: 10.1016/S0959-440X(03)00104-0.

(6) Kazlauskas, R. Engineering more stable proteins. *Chemical Society reviews* 2018, *47* (24), 9026-9045. DOI: 10.1039/c8cs00014j.

(7) Zhao, H. Effect of ions and other compatible solutes on enzyme activity, and its implication for biocatalysis using ionic liquids. *Journal of molecular catalysis. B, Enzymatic* 2005, *37* (1), 16-25. DOI: 10.1016/j.molcatb.2005.08.007.

(8) Patel, R.; Kumari, M.; Khan, A. B. Recent Advances in the Applications of Ionic Liquids in Protein Stability and Activity: A Review. *Applied Biochemistry and Biotechnology* 2014, *172* (8), 3701-3720. DOI: 10.1007/s12010-014-0813-6.

(9) Schindl, A.; Hagen, M. L.; Muzammal, S.; Gunasekera, H. A. D.; Croft, A. K. Proteins in ionic liquids: Reactions, applications, and futures. *Frontiers in chemistry* 2019, *7* (MAY), 347-347. DOI: 10.3389/fchem.2019.00347.

(10) Smiatek, J. Aqueous ionic liquids and their effects on protein structures: an overview on recent theoretical and experimental results. *Journal of physics. Condensed matter* 2017, *29* (23), 233001-233001.

(11) Borrell, K. L.; Cancglin, C.; Stinger, B. L.; DeFrates, K. G.; Caputo, G. A.; Wu, C.; Vaden, T. D. An Experimental and Molecular Dynamics Study of Red Fluorescent Protein mCherry in Novel Aqueous Amino Acid Ionic Liquids. *The journal of physical chemistry. B* 2017, *121* (18), 4823-4832. DOI: 10.1021/acs.jpcb.7b03582.

(12) Acharyya, A.; DiGiuseppi, D.; Stinger, B. L.; Schweitzer-Stenner, R.; Vaden, T. D. Structural Destabilization of Azurin by Imidazolium Chloride Ionic Liquids in Aqueous Solution. *The journal of physical chemistry. B* 2019, *123* (32), 6933-6945. DOI: 10.1021/acs.jpcb.9b04113.

(13) Patel, R.; Clark, A. K.; DeStefano, G.; DeStefano, I.; Gogoj, H.; Gray, E.; Patel, A. Y.; Hauner, J. T.; Caputo, G. A.; Vaden, T. D. Sequence-specific destabilization of azurin by tetramethylguanidinium-dipeptide ionic liquids. *Biochemistry and biophysics reports* 2022, *30*, 101242-101242. DOI: 10.1016/j.bbrep.2022.101242.

(14) Wu, W.; Han, B.; Gao, H.; Liu, Z.; Jiang, T.; Huang, J. Desulfurization of Flue Gas: SO2 Absorption by an Ionic Liquid. *Angewandte Chemie* 2004, *116* (18), 2469-2471. DOI: 10.1002/ange.200353437.

(15) Miao, S.; Atkin, R.; Warr, G. Design and applications of biocompatible choline amino acid ionic liquids. *Green Chemistry* 2022, *24* (19), 7281-7304, 10.1039/D2GC02282F. DOI: 10.1039/D2GC02282F.

(16) Clarke, C. J.; Tu, W.-C.; Levers, O.; Bröhl, A.; Hallett, J. P. Green and Sustainable Solvents in Chemical Processes. *Chemical reviews* 2018, *118* (2), 747-800. DOI: 10.1021/acs.chemrev.7b00571.

(17) Ding, X.; Wang, Y.; Zeng, Q.; Chen, J.; Huang, Y.; Xu, K. Design of functional guanidinium ionic liquid aqueous two-phase systems for the efficient purification of protein. *Analytica chimica acta* 2014, *815*, 22-32. DOI: 10.1016/j.aca.2014.01.030.

(18) Egorova, K. S.; Gordeev, E. G.; Ananikov, V. P. Biological Activity of Ionic Liquids and Their Application in Pharmaceutics and Medicine. *Chemical reviews* 2017, *117* (10), 7132-7189. DOI: 10.1021/acs.chemrev.6b00562.

(19) Md Moshikur, R.; Chowdhury, M. R.; Moniruzzaman, M.; Goto, M. Biocompatible ionic liquids and their applications in pharmaceutics. *Green chemistry : an international journal and green chemistry resource : GC* 2020, *22* (23), 8116-8139. DOI: 10.1039/d0gc02387f.

(20) Welton, T. Ionic liquids: a brief history. *Biophysical reviews* 2018, *10* (3), 691-706. DOI: 10.1007/s12551-018-0419-2.

(21) Tao, D.-J.; Cheng, Z.; Chen, F.-F.; Li, Z.-M.; Hu, N.; Chen, X.-S. Synthesis and Thermophysical Properties of Biocompatible Cholinium-Based Amino Acid Ionic Liquids. *Journal of chemical and engineering data* 2013, *58* (6), 1542-1548. DOI: 10.1021/je301103d.

(22) Weaver, K. D.; Kim, H. J.; Sun, J.; MacFarlane, D. R.; Elliott, G. D. Cyto-toxicity and biocompatibility of a family of choline phosphate ionic liquids designed for pharmaceutical applications. *Green chemistry : an international journal and green chemistry resource : GC* 2010, *12* (3), 507-551. DOI: 10.1039/b918726j.

(23) Mohammad, A.; Inamuddin, D. *Green Solvents II: Properties and Applications of Ionic Liquids*; Springer Netherlands, 2012. DOI: 10.1007/978-94-007-2891-2.

(24) Neidle, S. Quadruplex Nucleic Acids as Novel Therapeutic Targets. *Journal of Medicinal Chemistry* 2016, *59* (13), 5987-6011. DOI: 10.1021/acs.jmedchem.5b01835.

(25) Monsen, R. C.; Trent, J. O.; Chaires, J. B. G-quadruplex DNA: A Longer Story. *Accounts of chemical research* 2022, *55* (22), 3242-3252. DOI: 10.1021/acs.accounts.2c00519.

(26) Kosiol, N.; Juranek, S.; Brossart, P.; Heine, A.; Paeschke, K. G-quadruplexes: a promising target for cancer therapy. *Mol Cancer* 2021, *20* (1), 40. DOI: 10.1186/s12943-021-01328-4 From NLM.

(27) Simonsson, T. G-quadruplex DNA structures--variations on a theme. *Biol Chem* 2001, *382* (4), 621-628. DOI: 10.1515/BC.2001.073 From NLM Medline.

(28) Spiegel, J.; Adhikari, S.; Balasubramanian, S. The Structure and Function of DNA G-Quadruplexes. *Trends in Chemistry* 2020, *2* (2), 123-136. DOI: 10.1016/j.trechm.2019.07.002 (acccessed 2023/03/13).

(29) Hazel, P.; Huppert, J.; Balasubramanian, S.; Neidle, S. Loop-Length-Dependent Folding of G-Quadruplexes. *Journal of the American Chemical Society* 2004, *126* (50), 16405-16415. DOI: 10.1021/ja045154j.

(30) Lin, C.; Yang, D. Human Telomeric G-Quadruplex Structures and G-Quadruplex-Interactive Compounds. *Telomeres and Telomerase* 2017, 171-196. DOI: 10.1007/978-1-4939-6892-3_17.

(31) Brooks, T. A.; Hurley, L. H. Targeting MYC Expression through G-Quadruplexes. *Genes & Cancer* **2**010, *1* (6), 641-649. DOI: 10.1177/1947601910377493 (acccessed 2023/09/13).

(32) Ou, T.-M.; Lu, Y.-J.; Zhang, C.; Huang, Z.-S.; Wang, X.-D.; Tan, J.-H.; Chen, Y.; Ma, D.-L.; Wong, K.-Y.; Tang, J. C.-O.; et al. Stabilization of G-Quadruplex DNA and Down-Regulation of Oncogene c-myc by Quindoline Derivatives. *Journal of medicinal chemistry* 2007, *50* (7), 1465-1474. DOI: 10.1021/jm0610088.

(33) Kaulage, M. H.; Maji, B.; Pasadi, S.; Ali, A.; Bhattacharya, S.; Muniyappa, K. Targeting G-quadruplex DNA structures in the telomere and oncogene promoter regions by benzimidazole–carbazole ligands. *European Journal of Medicinal Chemistry* 2018, *148*, 178-194. DOI: https://doi.org/10.1016/j.ejmech.2018.01.091.

(34) Seenisamy, J.; Rezler, E. M.; Powell, T. J.; Tye, D.; Gokhale, V.; Joshi, C. S.; Siddiqui-Jain, A.; Hurley, L. H. The Dynamic Character of the G-Quadruplex Element in the c-MYC Promoter and Modification by TMPyP4. *Journal of the American Chemical Society* 2004, *126* (28), 8702-8709. DOI: 10.1021/ja040022b.

(35) Paradis, N. J.; Clark, A.; Gogoj, H.; Lakernick, P. M.; Vaden, T. D.; Wu, C. To probe the binding of TMPyP4 to c-MYC G-quadruplex with in water and in imidazolium-based ionic liquids using spectroscopy coupled with molecular dynamics simulations. *Journal of Molecular Liquids* 2022, *365*, 120097. DOI: https://doi.org/10.1016/j.molliq.2022.120097.

(36) Simonsson, T.; Kubista, M.; Pecinka, P. DNA tetraplex formation in the control region of c-myc. *Nucleic acids research* 1998, *26* (5), 1167-1172. DOI: 10.1093/nar/26.5.1167.

(37) Vorlíčková, M.; Kejnovská, I.; Bednářová, K.; Renčiuk, D.; Kypr, J. Circular Dichroism Spectroscopy of DNA: From Duplexes to Quadruplexes: CD SPECTROSCOPY OF DNA. *Chirality (New York, N.Y.)* 2012, *24* (9), 691-698. DOI: 10.1002/chir.22064.

(38) del Villar-Guerra, R.; Trent, J. O.; Chaires, J. B. G-Quadruplex Secondary Structure Obtained from Circular Dichroism Spectroscopy. *Angewandte Chemie (International ed.)* 2018, *57* (24), 7171-7175. DOI: 10.1002/anie.201709184.

(39) Agarwala, P.; Pandey, S.; Maiti, S. The tale of RNA G-quadruplex. *Organic & biomolecular chemistry* 2015, *13* (2), 557-5585. DOI: 10.1039/c4ob02681k.

(40) Qiu, M.; Tang, Y.; Chen, J.; Muriph, R.; Ye, Z.; Huang, C.; Evans, J.; Henske, E. P.; Xu, Q. Lung-selective mRNA delivery of synthetic lipid nanoparticles for the treatment of pulmonary lymphangioleiomyomatosis. *Proceedings of the National Academy of Sciences - PNAS* 2022, *119* (8), 1. DOI: 10.1073/pnas.2116271119.

(41) Quental, M. V.; Pedro, A. Q.; Pereira, P. c.; Sharma, M.; Queiroz, J. o. A.; Coutinho, J. o. A. P.; Sousa, F.; Freire, M. G. Integrated Extraction-Preservation Strategies for RNA Using Biobased Ionic Liquids. *ACS sustainable chemistry & engineering* 2019, *7* (10), 9439-9448. DOI: 10.1021/acssuschemeng.9b00688.

(42) Uddin, M. N.; Roni, M. A. Challenges of Storage and Stability of mRNA-Based COVID-19 Vaccines. *Vaccines* 2021, *9* (9), 1033.

(43) Saramago, M.; Bárria, C.; dos Santos, R. F.; Silva, I. J.; Pobre, V.; Domingues, S.; Andrade, J. M.; Viegas, S. C.; Arraiano, C. M. The role of RNases in the regulation of small RNAs. *Current Opinion in Microbiology* 2014, *18*, 105-115. DOI: https://doi.org/10.1016/j.mib.2014.02.009.

(44) Singh, U. K.; Kumari, M.; Khan, S. H.; Bohidar, H. B.; Patel, R. Mechanism and Dynamics of Long-Term Stability of Cytochrome c Conferred by Long-Chain Imidazolium Ionic Liquids at Low Concentration. *ACS sustainable chemistry & engineering* 2018, *6* (1), 803-815. DOI: 10.1021/acssuschemeng.7b03168.

(45) Sahoo, D. K.; Jena, S.; Tulsiyan, K. D.; Dutta, J.; Chakrabarty, S.; Biswal, H. S. Amino-Acid-Based Ionic Liquids for the Improvement in Stability and Activity of Cytochrome c: A Combined Experimental and Molecular Dynamics Study. *The journal of physical chemistry. B* 2019, *123* (47), 10100-10109. DOI: 10.1021/acs.jpcb.9b09278.

(46) Attri, P.; Venkatesu, P. Thermodynamic characterization of the biocompatible ionic liquid effects on protein model compounds and their functional groups. *Physical Chemistry Chemical Physics* 2011, *13* (14), 6566-6575, 10.1039/C0CP02768E. DOI: 10.1039/C0CP02768E.

(47) Vasantha, T.; Attri, P.; Venkatesu, P.; Devi, R. S. R. Structural Basis for the Enhanced Stability of Protein Model Compounds and Peptide Backbone Unit in Ammonium Ionic Liquids. *The Journal of Physical Chemistry B* 2012, *116* (39), 11968-11978. DOI: 10.1021/jp308443f.

(48) Miller, M. C.; Hanna, S. L.; DeFrates, K. G.; Fiebig, O. C.; Vaden, T. D. Kinetics and mass spectrometric measurements of myoglobin unfolding in aqueous ionic liquid solutions. *Int J Biol Macromol* 2016, *85*, 200-207. DOI: 10.1016/j.ijbiomac.2015.12.067 From NLM.

(49) Kumar Sahoo, D.; Devi Tulsiyan, K.; Jena, S.; Biswal, H. S. Implication of Threonine-Based Ionic Liquids on the Structural Stability, Binding and Activity of Cytochrome c. *Chemphyschem* 2020, *21* (23), 2525-2535. DOI: 10.1002/cphc.202000761 From NLM.

(50) DeStefano, I.; DeStefano, G.; Paradis, N. J.; Patel, R.; Clark, A. K.; Gogoj, H.; Singh, G.; Jonnalagadda, K. S.; Patel, A. Y.; Wu, C.; et al. Thermodynamic destabilization of azurin by four different tetramethylguanidinium amino acid ionic liquids. *International journal of biological macromolecules* 2021, *180*, 355-364. DOI: 10.1016/j.ijbiomac.2021.03.090.

(51) Gathergood, N.; Garcia, M. T.; Scammells, P. J. Biodegradable ionic liquids: Part I. Concept, preliminary targets and evaluation. *Green chemistry : an international journal and green chemistry resource : GC* 2004, *6* (3), 166-175. DOI: 10.1039/b315270g.

(52) Ohno, H.; Fukumoto, K. Amino Acid Ionic Liquids. *Accounts of chemical research* 2007, *40* (11), 1122-1129. DOI: 10.1021/ar700053z.

(53) Yang, Z. Hofmeister effects: an explanation for the impact of ionic liquids on biocatalysis. *Journal of biotechnology* 2009, *144* (1), 12-22. DOI: 10.1016/j.jbiotec.2009.04.011.

(54) Yang, Z.; Liu, X.-J.; Chen, C.; Halling, P. J. Hofmeister effects on activity and stability of alkaline phosphatase. *Biochimica et biophysica acta. Proteins and proteomics* 2010, *1804* (4), 821-828. DOI: 10.1016/j.bbapap.2009.12.005.

(55) Kumar, A.; Venkatesu, P. Does the stability of proteins in ionic liquids obey the Hofmeister series? *International journal of biological macromolecules* 2014, *63*, 244-253. DOI: 10.1016/j.ijbiomac.2013.10.031.

(56) De Santis, S.; Masci, G.; Casciotta, F.; Caminiti, R.; Scarpellini, E.; Campetella, M.; Gontrani, L. Cholinium-amino acid based ionic liquids: A new method of synthesis and physico-chemical characterization. *Physical chemistry chemical physics : PCCP* 2015, *17* (32), 20687-20698. DOI: 10.1039/c5cp01612f.

(57) Kohn, E. M.; Lee, J. Y.; Calabro, A.; Vaden, T. D.; Caputo, G. A. Heme Dissociation from Myoglobin in the Presence of the Zwitterionic Detergent N,N-Dimethyl-N-Dodecylglycine Betaine: Effects of Ionic Liquids. *Biomolecules* 2018, *8* (4), 126. DOI: 10.3390/biom8040126.

(58) Jha, I.; Attri, P.; Venkatesu, P. Unexpected effects of the alteration of structure and stability of myoglobin and hemoglobin in ammonium-based ionic liquids. *Physical chemistry chemical physics : PCCP* 2014, *16* (12), 5514-5526. DOI: 10.1039/c3cp54398f.

(59) Sarkar, S.; Singh, P. C. The combined action of cations and anions of ionic liquids modulates the formation and stability of G-quadruplex DNA. *Phys Chem Chem Phys* 2021, *23* (42), 24497-24504. DOI: 10.1039/d1cp03730g From NLM.

(60) Esperança, J. M. S. S.; Tariq, M.; Pereiro, A. B.; Araújo, J. M. M.; Seddon, K. R.; Rebelo, L. P. N. Anomalous and not-so-common behavior in common ionic liquids and ionic liquid-containing systems. *Frontiers in chemistry* 2019, *7*, 450-450. DOI: 10.3389/fchem.2019.00450.

(61) Kaur, G.; Kumar, H.; Singla, M. Diverse applications of ionic liquids: A comprehensive review. *Journal of Molecular Liquids* 2022, *351*, 118556. DOI: https://doi.org/10.1016/j.molliq.2022.118556.

(62) Curreri, A. M.; Mitragotri, S.; Tanner, E. E. L. Recent Advances in Ionic Liquids in Biomedicine. *Advanced science* 2021, *8* (17), e2004819-n/a. DOI: 10.1002/advs.202004819.

(63) Neilan, E. G.; Shih, V. E. Amino Acids. In *Encyclopedia of the Neurological Sciences*, Aminoff, M. J., Daroff, R. B. Eds.; Academic Press, 2003; pp 112-116.

(64) Scrosati, B.; Armand, M.; Endres, F.; MacFarlane, D. R.; Ohno, H. Ionic-liquid materials for the electrochemical challenges of the future. *Nature materials* 2009, *8* (8), 621-629. DOI: 10.1038/nmat2448.

(65) Petkovic, M.; Ferguson, J. L.; Gunaratne, H. Q. N.; Ferreira, R.; Leitão, M. C.; Seddon, K. R.; Rebelo, L. P. N.; Pereira, C. S. Novel biocompatible cholinium-based ionic liquids - Toxicity and biodegradability. *Green chemistry : an international journal and green chemistry resource : GC* 2010, *12* (4), 643-664. DOI: 10.1039/b922247b.

(66) Fukumoto, K.; Yoshizawa, M.; Ohno, H. Room Temperature Ionic Liquids from 20 Natural Amino Acids. *Journal of the American Chemical Society* 2005, *127* (8), 2398-2399. DOI: 10.1021/ja043451i.

(67) Shronts, E. P. Essential Nature of Choline with Implications for Total Parenteral Nutrition. *Journal of the American Dietetic Association* 1997, *97* (6), 639-649. DOI: https://doi.org/10.1016/S0002-8223(97)00161-2.

(68) Liu, Q.-P.; Hou, X.-D.; Li, N.; Zong, M.-H. Ionic liquids from renewable biomaterials: synthesis, characterization and application in the pretreatment of biomass. *Green Chemistry* 2012, *14* (2), 304-307, 10.1039/C2GC16128A. DOI: 10.1039/C2GC16128A.

(69) Stolte, S.; Arning, J.; Bottin-Weber, U.; Matzke, M.; Stock, F.; Thiele, K.; Uerdingen, M.; Welz-Biermann, U.; Jastorff, B.; Ranke, J. Anion effects on the cytotoxicity of ionic liquids. *Green chemistry : an international journal and green chemistry resource : GC* 2006, *8* (7), 621-629. DOI: 10.1039/b602161a.

(70) Pernak, J.; Sobaszkiewicz, K.; Mirska, I. Anti-microbial activities of ionic liquids. *Green chemistry : an international journal and green chemistry resource : GC* 2003, *5* (1), 52-56. DOI: 10.1039/b207543c.

(71) Zhu, A.; Wang, M.; Li, L.; Wang, J. Tetramethylguanidium-based ionic liquids as efficient and reusable catalysts for the synthesis of biscoumarin at room temperature. *RSC advances* 2015, *5* (90), 73974-73979. DOI: 10.1039/c5ra14247d.

(72) Pratap Singh, A.; Sithambaram, D.; Sanghavi, R.; Kumar Gupta, P.; Shanker Verma, R.; Doble, M.; Gardas, R. L.; Senapati, S. Environmentally benign tetramethylguanidinium cation based ionic liquids. *New journal of chemistry* 2017, *41* (20), 12268-12277. DOI: 10.1039/c7nj03167j.

(73) Earle, M. J.; Gordon, C. M.; Plechkova, N. V.; Seddon, K. R.; Welton, T. Decolorization of Ionic Liquids for Spectroscopy. *Analytical chemistry (Washington)* 2007, *79* (2), 758-764. DOI: 10.1021/ac061481t.

(74) Patel, A. Y.; Jonnalagadda, K. S.; Paradis, N.; Vaden, T. D.; Wu, C.; Caputo, G. A. Effects of ionic liquids on metalloproteins. *Molecules (Basel, Switzerland)* 2021, *26* (2), 514. DOI: 10.3390/molecules26020514.

(75) Zamiri, B.; Reddy, K.; Macgregor, R. B.; Pearson, C. E. TMPyP4 porphyrin distorts RNA G-quadruplex structures of the disease-associated r(GGGGCC)n repeat of the C9orf72 gene and blocks interaction of RNAbinding proteins. *The Journal of biological chemistry* 2014, *289* (8), 4653-4659. DOI: 10.1074/jbc.C113.502336.

(76) Kelly, S. M.; Jess, T. J.; Price, N. C. How to study proteins by circular dichroism. *Biochimica et biophysica acta. Proteins and proteomics* 2005, *1751* (2), 119-139. DOI: 10.1016/j.bbapap.2005.06.005.

(77) Remington, S. J. Green fluorescent protein: A perspective. *Protein science* 2011, *20* (9), 1509-1519. DOI: 10.1002/pro.684.

(78) Hasegawa, J.-y.; Ise, T.; Fujimoto, K. J.; Kikuchi, A.; Fukumura, E.; Miyawaki, A.; Shiro, Y. Excited States of Fluorescent Proteins, mKO and DsRed: Chromophore−Protein Electrostatic Interaction Behind the Color Variations. *The journal of physical chemistry. B* 2010, *114* (8), 2971-2979. DOI: 10.1021/jp9099573.

(79) Kirchner, B.; Perlt, E. Proteins in Ionic Liquids: Current Status of Experiments and Simulations. Topics in Current Chemistry Collections, Springer International Publishing AG, 2018; pp 127-152.

(80) Tavares, A. P. M.; Rodriguez, O.; Macedo, E. A. Ionic liquids as alternative co-solvents for laccase: Study of enzyme activity and stability. *Biotechnology and bioengineering* 2008, *101* (1), 201-207. DOI: 10.1002/bit.21866.

(81) Patel, A. Y.; Clark, A. K.; Paradis, N. J.; Amin, M.; Vaden, T. D.; Wu, C.; Caputo, G. A. Effects of Ionic Liquids on Laccase from Trametes versicolor. *Biophysica* 2021, *1* (4), 429-444. DOI: 10.3390/biophysica1040031.

(82) Pucci, F.; Rooman, M. Physical and molecular bases of protein thermal stability and cold adaptation. *Current opinion in structural biology* 2017, *42*, 117-128. DOI: 10.1016/j.sbi.2016.12.007.

(83) Myers, J. K.; Pace, C. N. Hydrogen bonding stabilizes globular proteins. *Biophysical journal* 1996, *71* (4), 2033-2039. DOI: 10.1016/S0006-3495(96)79401-8.

(84) Hung, C.-L.; Kuo, Y.-H.; Lee, S. W.; Chiang, Y.-W. Protein Stability Depends Critically on the Surface Hydrogen-Bonding Network: A Case Study of Bid Protein. *The journal of physical chemistry. B* 2021, *125* (30), 8373-8382. DOI: 10.1021/acs.jpcb.1c03245.

(85) Shi, Z.; Krantz, B. A.; Kallenbach, N.; Sosnick, T. R. Contribution of Hydrogen Bonding to Protein Stability Estimated from Isotope Effects. *Biochemistry (Easton)* 2002, *41* (7), 2120-2129. DOI: 10.1021/bi011307t.

(86) Constantinescu, D.; Weingärtner, H.; Herrmann, C. Protein Denaturation by Ionic Liquids and the Hofmeister Series: A Case Study of Aqueous Solutions of Ribonuclease A. *Angewandte Chemie (International ed.)* 2007, *46* (46), 8887-8889. DOI: 10.1002/anie.200702295.

(87) Scholtz, J. M.; York, E. J.; Stewart, J. M.; Baldwin, R. L. A neutral, water-soluble, .alpha.-helical peptide: the effect of ionic strength on the helix-coil equilibrium. *Journal of the American Chemical Society* 1991, *113* (13), 5102-5104. DOI: 10.1021/ja00013a079.

(88) Dominy, B. N.; Perl, D.; Schmid, F. X.; Brooks, C. L. The Effects of Ionic Strength on Protein Stability: The Cold Shock Protein Family. *Journal of molecular biology* 2002, *319* (2), 541-554. DOI: 10.1016/S0022-2836(02)00259-0.

(89) Barbier, M.; Damron, F. H.; Bielecki, P.; Suárez-Diez, M.; Puchałka, J.; Albertí, S.; dos Santos, V. M.; Goldberg, J. B. From the Environment to the Host: Re-Wiring of the Transcriptome of Pseudomonas aeruginosa from 22°C to 37°C. *PLOS ONE* 2014, *9* (2), e89941. DOI: 10.1371/journal.pone.0089941.

(90) Vacas, A.; Sugden, C.; Velasco-Rodriguez, Ó.; Algarabel-Olona, M.; Peña-Guerrero, J.; Larrea, E.; Fernández-Rubio, C.; Nguewa, P. A. Construction of Two mCherry Plasmids (pXG-mCherry) for Transgenic Leishmania: Valuable Tools for Future Molecular Analysis. *Journal of Parasitology Research* 2017, *2017*, 1964531-1964511. DOI: 10.1155/2017/1964531.

(91) Cloin, B. M. C.; De Zitter, E.; Salas, D.; Gielen, V.; Folkers, G. E.; Mikhaylova, M.; Bergeler, M.; Krajnik, B.; Harvey, J.; Hoogenraad, C. C.; et al. Efficient switching of mCherry fluorescence using chemical caging. *Proceedings of the National Academy of Sciences* 2017, *114* (27), 7013-7018. DOI: doi:10.1073/pnas.1617280114.

(92) Krishna Deepak, R. N. V.; Sankararamakrishnan, R. Unconventional N-H...N Hydrogen Bonds Involving Proline Backbone Nitrogen in Protein Structures. *Biophysical journal* 2016, *110* (9), 1967-1979. DOI: 10.1016/j.bpj.2016.03.034.

(93) Fitter, J. A Measure of Conformational Entropy Change during Thermal Protein Unfolding Using Neutron Spectroscopy. *Biophysical Journal* 2003, *84* (6), 3924-3930. DOI: 10.1016/s0006-3495(03)75120-0.

(94) Olejko, L.; Dutta, A.; Shahsavar, K.; Bald, I. Influence of Different Salts on the G-Quadruplex Structure Formed from the Reversed Human Telomeric DNA Sequence. *International journal of molecular sciences* 2022, *23* (20), 12206. DOI: 10.3390/ijms232012206.

(95) Bhattacharyya, D.; Mirihana Arachchilage, G.; Basu, S. Metal Cations in G-Quadruplex Folding and Stability. *Frontiers in chemistry* 2016, *4*, 38-38. DOI: 10.3389/fchem.2016.00038.

(96) Gu, J.; Leszczynski, J. Origin of Na+/K+ Selectivity of the Guanine Tetraplexes in Water: The Theoretical Rationale. *The journal of physical chemistry. A, Molecules, spectroscopy, kinetics, environment, & general theory* 2002, *106* (3), 529-532. DOI: 10.1021/jp012739g.

(97) Łuczak, J.; Hupka, J.; Thöming, J.; Jungnickel, C. Self-organization of imidazolium ionic liquids in aqueous solution. *Colloids and surfaces. A, Physicochemical and engineering aspects* 2008, *329* (3), 125-133. DOI: 10.1016/j.colsurfa.2008.07.012.

(98) Jungnickel, C.; Łuczak, J.; Ranke, J.; Fernández, J. F.; Müller, A.; Thöming, J. Micelle formation of imidazolium ionic liquids in aqueous solution. *Colloids and surfaces. A, Physicochemical and engineering aspects* 2008, *316* (1), 278-284. DOI: 10.1016/j.colsurfa.2007.09.020.

(99) Qiu, M.; Glass, Z.; Xu, Q. Nonviral Nanoparticles for CRISPR-Based Genome Editing: Is It Just a Simple Adaption of What Have Been Developed for Nucleic Acid Delivery? *Biomacromolecules* 2019, *20* (9), 3333-3339. DOI: 10.1021/acs.biomac.9b00783.

(100) Foulk, M. S.; Urban, J. M.; Casella, C.; Gerbi, S. A. Characterizing and controlling intrinsic biases of lambda exonuclease in nascent strand sequencing reveals phasing between nucleosomes and G-quadruplex motifs around a subset of human replication origins. *Genome Res* 2015, *25* (5), 725-735. DOI: 10.1101/gr.183848.114 From NLM.

(101) Hald Albertsen, C.; Kulkarni, J. A.; Witzigmann, D.; Lind, M.; Petersson, K.; Simonsen, J. B. The role of lipid components in lipid nanoparticles for vaccines and gene therapy. *Advanced drug delivery reviews* 2022, *188*, 114416-114416. DOI: 10.1016/j.addr.2022.114416.

(102) Kis, Z. Stability Modelling of mRNA Vaccine Quality Based on Temperature Monitoring throughout the Distribution Chain. *Pharmaceutics* 2022, *14* (2), 430. DOI: 10.3390/pharmaceutics14020430.

(103) Silva, M.; Figueiredo, A. M.; Cabrita, E. J. Epitope mapping of imidazolium cations in ionic liquid-protein interactions unveils the balance between hydrophobicity and electrostatics towards protein destabilisation. *Physical chemistry chemical physics : PCCP* 2014, *16* (42), 23394-23403. DOI: 10.1039/c4cp03534h.